Retrovirology

BioMed Central

Research

Open Access

Synergistic effect of human CycT1 and CRM1 on HIV-1 propagation in rat T cells and macrophages

Hiroyuki Okada[1], Xianfeng Zhang[1], Ismael Ben Fofana[1,2], Mika Nagai[1], Hajime Suzuki[1], Takashi Ohashi[1] and Hisatoshi Shida*[1]

Address: [1]Institute for Genetic Medicine, Hokkaido University, Kita-ku, Sapporo 060-0815, Japan and [2]Microbiology Division, New England Primate Research Center, Harvard Medical School, One Pine Hill Drive, Southborough, Maryland 01772, USA

Email: Hiroyuki Okada - hiro1230@igm.hokudai.ac.jp; Xianfeng Zhang - zhangxf@igm.hokudai.ac.jp; Ismael Ben Fofana - Ismael_Fofana@hms.harvard.edu; Mika Nagai - purefood@igm.hokudai.ac.jp; Hajime Suzuki - hjsuzuki@igm.hokudai.ac.jp; Takashi Ohashi - ohashi-t@igm.hokudai.ac.jp; Hisatoshi Shida* - hshida@igm.hokudai.ac.jp

* Corresponding author

Published: 12 May 2009

Retrovirology 2009, **6**:43 doi:10.1186/1742-4690-6-43

Received: 11 September 2008
Accepted: 12 May 2009

This article is available from: http://www.retrovirology.com/content/6/1/43

Abstract

Background: *In vivo* studies of HIV-1 pathogenesis and testing of antiviral strategies have been hampered by the lack of an immunocompetent small animal model that is highly susceptible to HIV-1 infection. Although transgenic rats that express the HIV-1 receptor complex hCD4 and hCCR5 are susceptible to infection, HIV-1 replicates very poorly in these animals. To demonstrate the molecular basis for developing a better rat model for HIV-1 infection, we evaluated the effect of human CyclinT1 (hCycT1) and CRM1 (hCRM1) on Gag p24 production in rat T cells and macrophages using both established cell lines and primary cells prepared from hCycT1/hCRM1 transgenic rats.

Results: Expression of hCycT1 augmented Gag production 20–50 fold in rat T cells, but had little effect in macrophages. Expression of hCRM1 enhanced Gag production 10–15 fold in macrophages, but only marginally in T cells. Expression of both factors synergistically enhanced p24 production to levels approximately 10–40% of those detected in human cells. R5 viruses produced in rat T cells and macrophages were fully infectious.

Conclusion: The expression of both hCycT1 and hCRM1 appears to be fundamental to developing a rat model that supports robust propagation of HIV-1.

Background

A small-animal model of HIV-1 infection is needed for development of prophylactic vaccines and more efficient antiviral therapies. Current animal models of HIV infection, including non-human primates [1-4] and severe combined immunodeficiency (SCID) mice transplanted with fetal human cells [5,6], have made significant contributions to our understanding of lentiviral pathogenesis and to the development of vaccines and therapeutic agents. However, these models have shortcomings, such as their limited availability and high cost, their permissivity restricted to related retroviruses of nonhuman primates, as well as the absence or insufficient induction of an immune response against HIV-1. Therefore, a better small-animal model is needed.

Rodents may be useful models if they can be infected with HIV-1. Because they are established experimental animals,

inbred strains are available, and genetic manipulations can be performed. However, a fully permissive model has not been developed yet because of several inherent blocks to HIV-1 replication in rodent cells. One major block to HIV-1 replication is at the level of viral entry into the cell; this may be overcome by introducing human CD4 (hCD4) and CCR5 (hCCR5) [7,8]. Indeed, transgenic (Tg) rats expressing these receptors support some HIV-1 replication, albeit poorly [8], whereas Tg mice expressing hCD4 and hCCR5 do not support any HIV replication [9]. These results suggest that rats may provide a good small-animal model.

Studies on rodent cell-specific defects in the HIV-1 life cycle after viral entry provide the molecular basis for improving the propagation of HIV in rodents. However, several studies using established cells lines [7,10,11] have indicated that there are cell line specific defects in each step of the viral life cycle. Moreover, technical difficulties have hampered detailed analyses of the function of cellular cofactors in rodent T cells and macrophages, particularly primary cells.

A study of the effects of rodent cellular factors on the function of the viral factors Tat and Rev will be of importance because of the essential roles these proteins play in viral propagation. Currently, controversial results have been reported regarding the existence of a profound block affecting Tat function in rodent cells. In early studies, human CyclinT1 (hCycT1), identified as a Tat interacting protein that is crucial for transcription during HIV-1 replication [12], was expressed in mouse NIH 3T3 fibroblasts and transcriptional activity was dramatically enhanced [13,14]. Moreover, hCycT1 Tg mice supported the enhanced expression of an integrated HIV-1 provirus [15]. A single amino acid difference between human and mouse CyclinT1 (mCycT1), which has a tyrosine at residue 261 in place of the cysteine amino acid in hCycT1, causes almost a complete loss of Tat cofactor activity [13,14]. In contrast to mouse cells, rat cells support significant amounts of Tat function, even though rat CyclinT1 (rCycT1) has a tyrosine at residue 261 and shares ~96% sequence homology with mCycT1. Only 2–5 fold enhancement of Tat function by overexpression of hCycT1 in rat cells has been reported. Moreover, since the reported experiments lacked the expression of rCycT1 as a control, uncertainty remains whether it was the quantity or the quality of exogenously-expressed hCycT1 which augmented Tat function [7,16,17]. On the other hand, a substantial increase in Gag protein levels upon hCycT1 expression in a rat myelomonocytic precursor cell line has been reported [18].

Rev function is involved in the expression of the unspliced 9-Kb and partially-spliced 4-Kb RNAs that encode the HIV viral genome and the structural proteins [19]. Rev activity that supports HIV-1 replication in rodent cells has also been debated, although a reduction in the ratio of the unspliced 9-kb transcript to the fully-spliced 2-kb viral transcript in rodent cells has generally been reported [7,10]. Moreover, the role of the rat counterpart of hCRM1, which exports HIV RNAs in cooperation with Rev [20,21], has been incompletely explored. Instead, oversplicing or a reduced stability of unspliced transcripts in rodent cells compared to human cells has been proposed [22], which has been reported to be repaired by the expression of the human p32 protein [23].

In this study, we investigated the effect of human CyclinT1 and CRM1 expressed in rat T cells and macrophages, including primary cells, in order to identify a molecular basis for improving a rat model for HIV-1 infection. Our results show that co-expression of hCycT1 and hCRM1 synergistically promotes Gag p24 production. Interestingly, cell type specific requirements for these two human factors were detected.

Methods

Cells and plasmids

Rat T cell lines, FPM1 [25] and C58(NT)D (ATCC TIB-236), a rat macrophage line, NR8383 (ATCC CRL-2192), and human T cell lines, Jurkat and Molt4R5, were used for propagation of HIV-1. TZM-bl cells were used to measure the infectivity of HIV-1 according to previously described procedures [26]. NR8383hCRM1, FPM1hCRM1, FPM1hCT, and FPM1hCT/hCRM1 expressing hCRM1, hCycT1, or both were constructed as described previously [40].

To construct hemagglutinin (HA)-tagged hCycT1, pβCycT, which harbors the human cyclinT1 cDNA in the pCXN2 vector, was used as a template for PCR with forward (5'-ggtctagagcactatggagggagagaggaag-3') and reverse (5'-gggaattcatgcatagtctggtacatcgtaggggtacttaggaaggggt-ggaagtggtgg-3') primers with the following amplification conditions: 2 min at 94°C, 30 cycles of 30 s at 94°C, 60 s at 64°C, 2.5 min at 72°C, and a final extension for 10 min at 72°C. The amplified DNA was digested and inserted between the *Eco*RI and *Xba*I sites of pCXN2 [41].

Rat Cyclin T1 mRNA was extracted from rat ER-1 neo1 cells using the Absolute RNA extraction Kit (Stratagene) and amplified by RT-PCR using the following primers: 5'-ccgaattcaagcactatggagggagagaggaa-3' and 5'-ccgaattcatg catagtctggtacatcgtaggggtacttaggaagaggtggaagaggtgg-3'. The amplification conditions were: 94°C for 2 min, 30 cycles of 15 s at 94°C, 30s at 60°C, 2.5 min at 68°C, and a final extension for 5 min at 68°C. The amplified DNA was digested and inserted into the *Eco*RI site of pCXN2.

To construct pSRαrCRM1-HA, pSRαrCRM1 was used for PCR with the following primers: 5'-ctggaatcacttggcagct-

gagctctacagagagagtcca-3' and 5'-tatggtaccttaagcataatcaggaacatcgtatgggtagtcacacatttcttct-gggatttc-3'. The amplification conditions were: 2 min at 94°C, 20 cycles of 30 s at 94°C, 1 min at 62°C, 2 min at 68°C, and a final extension for 10 min at 68°C. The amplified DNA was digested and inserted into the SacI and KpnI sites of pSRαrCRM1.

The following plasmids were used in this study: pSRα296 [42]; pCRRE [35]; pΔpol [24]; pMaxGFP (Amaxa) and pCDMβ-gal [43]; pNL4-3 [30]; pYU-2 [28]; p89.6 [32]; pLAI-2 [31]; pYK-JRCSF [27]; and pNLAD8-EGFP [29]. pH1-luc (a gift from Dr. A. Adachi) contains a luciferase coding sequence downstream of the HIV-1 LTR. pSRαhCRM1-HA was a gift from Dr. T. Kimura.

Development of Human Cyclin T1 Transgenic (Tg) Rats

An hCycT1 BAC (RZPD;RZPDB737F032099D) was microinjected into fertilized rat (F344) eggs. To identify Tg rats, total genomic DNA extracted from rat tail snips was examined by PCR using two sets of PCR primers with one primer annealing the BAC backbone vector and the other annealing the 5' or 3' end of hCyclin T1 genomic DNA. Primers CTB3 (gccaacgctcaatccggttctcgc) and CTGB3 (gctattttccagctgttctcgagtg) were used for the 5' end. Primers CTB4 (ttattccctagtccaaggatgac) and CTGB4 (cagacaatagactatcaagacactgtg) were used for the 3' end. PCR was performed using 500 ng of DNA as a template with the following amplification conditions: 94°C for 2 min, 30 cycles of denaturation (94°C for 1 min), annealing (58°C for the 5' end primers and 54°C for the 3' end primers, 30s), extension (72°C, 1 min), and a final extension (72°C, 5 min).

Preparation of rat primary cells and human cells

Rat primary T cells were enriched from splenocytes using a nylon wool column. More than 95% of the cells were $CD3^+$ cells, as evaluated by Flow Cytometry (FACS Calibur; Becton Dickinson). The cells were stimulated for 2 days with an anti-rat CD3 mAb (5 μg/ml) and an anti-rat CD28 mAb (0.5 μg/ml) that had been coated on the culture plates. $CD4^+$T cells were then isolated by negative selection using anti-rat CD8 MicroBeads (Miltenyi Biotec). Isolated $CD4^+CD8^-$T cells were >90% pure, as determined by staining with anti-rat-CD4 (BD Biosciences Pharmingen) and anti-rat-CD8 (BD Biosciences Pharmingen).

Rat peritoneal macrophages were isolated from rats that had been treated with 3% thioglycollate for 3 days. The macrophages were coated with anti-rat CD11b and isolated using goat anti-mouse IgG MicroBeads (Miltenyi Biotec). Isolated $CD11b^+$ peritoneal cells were >90% pure, as determined by staining with mouse anti-rat-ED2 (BD Biosciences). Isolated $CD11b^+$ $ED2^+$ peritoneal cells were cultured for 2 h at 37°C to allow them to adhere to the plates.

Human peripheral blood mononuclear cells (PBMCs) were isolated from healthy donors using Ficoll Paque Plus (Amersham Biotechnology) density centrifugation. The cells were activated with 5 μg/ml phytohemagglutinin-P (PHA-P) (SIGMA) and 20 U/ml IL-2 (PeproTech EC) for 3 days at 37°C. Peripheral blood lymphocytes (hPBLs) were harvested as non-adherent cells.

Human monocytes were isolated from PBMCs using anti-CD14 conjugated to magnetic beads (Miltenyi Biotec), and allowed to adhere on dishes at 37°C for 1 h in RPMI 1640 supplemented with 1% human serum. Human monocyte-derived macrophages (MDMs) were then generated by incubation in RPMI 1640 supplemented with 15% FBS, antibiotics, and GM-CSF (10 U/ml) (R & D) for 5 days.

Electroporation

Cell lines (2×10^6) and primary T cells (1×10^7) were electroporated in 100 μl of Nucleofector Solution (Cell line Solution V, Mouse T cell and human T cell Nucleofector kit, Amaxa Biosystems,) using the conditions (FPM1;T-03, C58(NT)D;T-20, NR8383;T-27, and rat primary T;X-01, Jurkat;X-01, Molt4R5;A-30, hPBL;U-14) and plasmids described in the Figure Legends. After 48 h, p24 in the supernatant and in cells was quantified using a p24 ELISA kit (Zeptometrix). In some cases, the viruses were concentrated by centrifugation at 15,000 rpm for 90 min in a microcentrifuge and p24 was quantitatively recovered from the pellets.

Western Blotting

Cells were lysed in buffer containing 10 mM Tris-HCl, pH 7.4, 1 mM $MgCl_2$, 0.5% NP40, and protease inhibitors or sample buffer without mercaptoethanol and dye, and protein concentrations were determined by BCA assay. Samples containing 50 μg protein were then subjected to Western blotting using anti-CycT1 (Novocastra Laboratories Ltd), anti-CRM1 [42], anti-HA (Behringer), or anti-β-actin (SIGMA).

Infection

Rat peritoneal macrophages and human MDMs were seeded at a density of 5×10^5 cells/well in 24 well plates and cultured for 1 day at 37°C. Macrophages were then inoculated with VSV-G-coated NL43 and NLAD8-EGFP (50 ng), which were prepared by transfection of pNL4-3 or pNLAD8-EGFP along with pVSV-G to 293 T cells with Fugene6, in the absence or presence of 20 μM PMPA [44] overnight at 37°C. Finally, cells were washed gently 5 times and 2 ml of RPMI containing 15% FCS with or without PMPA was added.

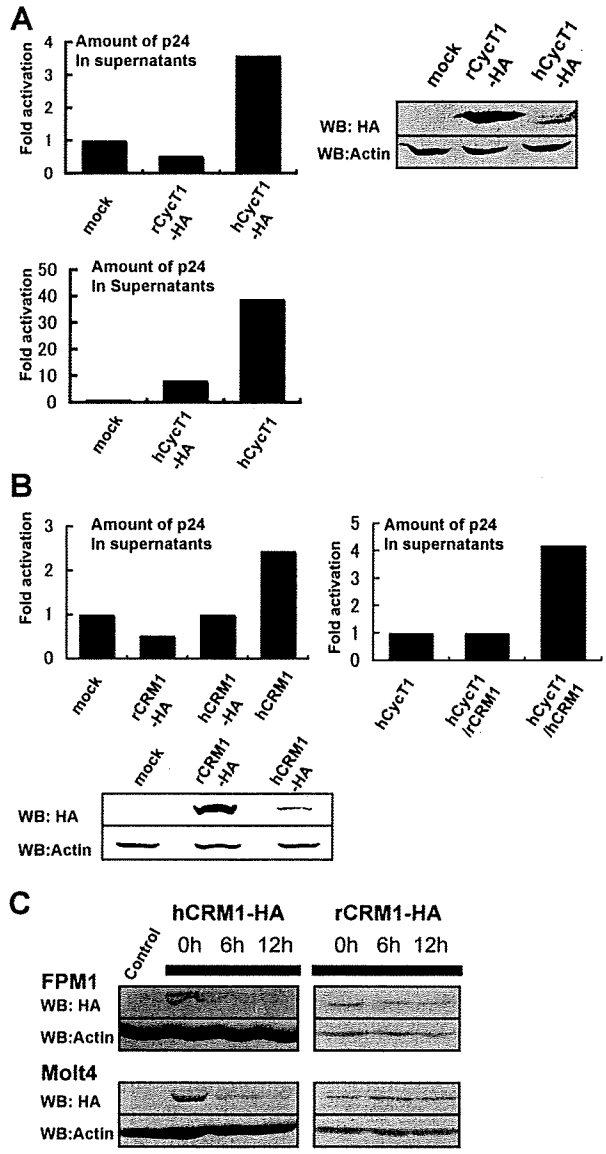

Figure 1

Effect of hCycT1 and hCRM1 expression in rat T cell lines (part 1). (A) FPM1 cells were electroporated with 2 μg pΔpol, 1 μg pMax-GFP, and 1 μg pCXN2, pCXN2hCycT1-HA, pβhCycT1, or pCXN2rCycT1-HA. After 2 days, p24 levels in the medium were measured by ELISA. The percentage of living cells was approximately 18% and approximately 95% of the living cells were GFP+ based on FACS analysis. The ratio of p24 in the CycT1 containing samples relative to mock treated samples was calculated. The total amount of p24 in the hCycT-HA containing sample was 119 pg. Values are means of duplicate samples. rCycT1 and hCycT1 were detected by Western blotting using anti-HA. (B) FPM1 cells were electroporated with 2 μg pΔpol, 1 μg pMax-GFP, and 0.5 μg pSRα296, pSRα hCRM1-HA, pSRαrCRM1-HA, or pSRαhCRM1. The percentage of living cells was approximately 4%, and 60% of the living cells were GFP+. The total amount of p24 in the sample containing hCRM1 was 146 pg. In the right panel, 1 μg pCNXhCycT1 was included. Values are means of duplicate samples. The total amount of p24 in the sample containing hCRM1 was 15.7 ng. (C) pSRα296, pSRαhCRM1-HA, or pSRαrCRM1-HA (0.5 μg) were electroporated into FPM1 and Molt4 cells, and 50 μg/ml cycloheximide was added after 24 h. The cells were then collected at 0, 6, and 12 h after the drug addition, and analyzed by Western blotting. Various amounts of the cell lysates were used for blotting (25 μg of hCRM1-HA containing FPM1, 5 μg rCRM1-HA containing FPM1, and 25 μg of hCRM1-HA or 10 μg of rCRM1-HA containing Molt4, respectively).

Results

Synergistic Effects of hCycT1 and hCRM1 in Rat T cell lines

Since controversial results regarding the activity of Tat in rat cells have been reported, we compared the effect of hCycT1 versus rCycT1expression in rat T cells. To express the HIV-1 genome and CycT1 in rat T cells, we used the electroporation of CycT1 and an HIV-1 genome expressing plasmid, since we experienced very low rates of HIV-1 infection even with VSV-G coated particles. In our hands, electroporation was the only way to introduce enough HIV genome into rat T cells. We co-electroporated pMax-GFP or pCDM-βgal to monitor the efficiency of electroporation. When we electroporated pΔpol, which was constructed by deleting 328 base pairs in the pol gene of the infectious pNL43 genome [24], and HA-tagged hCycT1 or rCycT1 into FPM1 cells, a rat $CD4^+$ T cell line transformed with HTLV-1 [25], Gag p24 production was enhanced several fold in the presence of hCycT1-HA. However, hCycT1 expression was very low. In contrast, rCycT1-HA was efficiently expressed, but did not alter Gag p24 production. Since hCycT1-HA may be unstable, we next used an untagged hCycT1 for co-electroporation. We detected a 40 fold enhancement of Gag production in the presence of hCycT1 (Fig. 1A). The band corresponding to hCycT1 was, however, hardly detected by Western blot analysis (data not shown). The reason why untagged hCycT1 enhanced expression more efficiently than hCycT1-HA is currently unclear, because the intracellular amounts of these hCycT1s cannot be exactly compared due to the different abilities of the anti-HA mAb and anti-hCycT1 antibody.

Next, to assess Rev activity in rat T cells, we compared the effects of hCRM1 and rCRM1 on HIV-1 propagation. When we electroporated HA-tagged CRM1 expression plasmids and pΔpol into FPM1 cells, p24 production was not significantly increased. The level of hCRM1-HA detected by Western blotting was very low. However, we reproducibly observed a 2–4 fold enhancement of p24 production in cells transiently expressing untagged hCRM1, but not rCRM1 (Fig. 1B). These results suggest that endogenous rCRM1 supports p24 production less efficiently than the hCRM1 and that Rev function is not absolutely blocked in rat T cells. To examine the stability of CRM1-HA, we added cycloheximide to inhibit translation in CRM1-transfected T cells and examined CRM1 protein levels over time. In both rat and human T cells, hCRM1-HA was much less stable than rCRM1-HA (Fig. 1C), partly accounting for the lower amounts of hCRM1 (See Fig. 1B).

To examine the effects of both hCycT1 and hCRM1 on HIV-1 propagation in rat T cells, including FPM1 and C58(NT)D cells, we co-electroporated these expression plasmids with pΔpol. Additionally, we co-transfected pH1-Luc, which expresses the luciferase gene driven by the HIV-1 LTR, to examine the effect of hCycT1 and hCRM1 on Tat-directed gene expression. Expression of hCycT1, but not hCRM1, enhanced LTR-derived expression several fold, consistent with the previously reported functions of these proteins. Notably, the enhancement of p24 production by hCycT1 was substantially greater than that of the luciferase activity. Furthermore, levels of extracellular p24 were more enriched than intracellular levels, and hCycT1 synergistically cooperated with hCRM1 to augment the synthesis of p24 by approximately 100 fold (Fig. 2A and 2B). These results suggest that hCycT1 enhanced the transcription of the LTR-driven HIV-1 pre-mRNA. Since the pre-mRNA is the source of mRNAs encoding Gag, Tat and Rev, its increase may trigger positive feedback in the synthesis of HIV-1 pre-mRNA as a result of increased Tat protein levels and in the amounts of unspliced mRNA as a result of increased Rev protein levels. Thus, Gag would be produced much more efficiently than luciferase. Subsequently, the enhanced Gag expression facilitates the more efficient release of viral particles. The level of p24 produced by rat T cells expressing both hCycT1 and hCRM1 was approximately 25–33% of the levels produced by the human T cell line Molt4 (data not shown).

To examine the effect of hCycT1 and hCRM1 on HIV-1 propagation using a full length HIV-1 clone, we electroporated pNL4-3 into FPM1 T cells that continuously expressed hCycT1 and hCRM1, and then quantified the production of p24. Again, hCycT1 greatly augmented p24 production, and hCRM1 had a moderate effect. Notably, the levels of hCycT1 and hCRM1 expression in FPM1 cells were similar to those in Molt4 cells (Fig. 2C). Thus, expression of these human factors should support robust HIV-1 propagation in rat T cells.

Synergistic Effects of hCycT1 and hCRM1 in rat macrophages

We examined the effect of hCycT1 and hCRM1 on p24 production and LTR-driven expression in the rat macrophage cell line NR8383, using the experimental approaches described above. Transient expression of rCRM1-HA in NR8383 cells did not affect p24 production, whereas hCRM1-HA enhanced p24 production 5–10 fold, although the level of hCRM1-HA expression was much less than that of rCRM1-HA (Fig. 3A). Expression of hCycT1 enhanced p24 production by only a few fold. The expression of hCycT1 was readily detected by Western blotting (Fig. 3B), in contrast to the low levels in rat T cells. Neither hCycT1 nor hCRM1 expression significantly affected luciferase expression driven by the HIV LTR (Fig. 3C). We also detected a greater than 10 fold enhancement of extracellular and intracellular p24 production in the presence of untagged hCRM1 (Fig. 3C), but not rCRM1 (data not shown). When hCycT1 and hCRM1 were co-expressed, they synergistically augmented p24 production

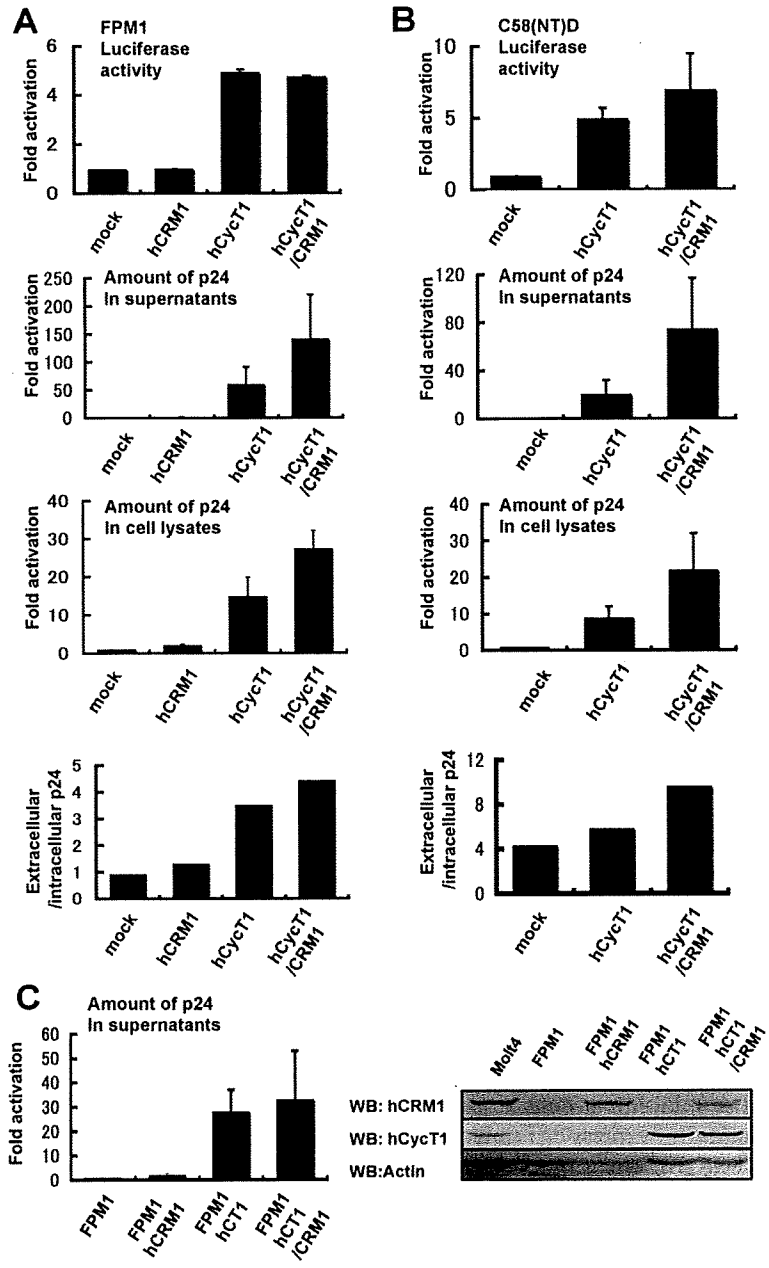

Figure 2
Effect of hCycT1 and hCRM1 expression in rat T cell lines (part 2). (A) FPM1 and (B) C58(NT)D cells were electroporated, as above, with the exception that 0.4 μg pH1-Luc and 0.2 μg pCDMβ-gal were used instead of pMax-GFP. LTR activity and transfection efficiency were measured by luciferase and β-gal assays using cell lysates. The luciferase/β-gal activity or the amount of p24 was calculated, and the value of the mock sample was normalized to 1. Values are means of triplicate samples and the SD was calculated. The amount of p24 in the FPM1 and C58(NT)D samples containing hCycT1/hCRM1 was 3.7 and 2.8 ng, respectively. (C) FPM1 cells continuously expressing hCycT1 and hCRM1 were electroporated with 4 μg pNL4-3 and 1 μg pMaxGFP. The percentage of living cells was approximately 10%, and 50% of the living cells were GFP+. The amount of p24 in the FPM1hCT/hCRM1 sample was 6.0 ng. Approximately 10 μg of each cell lysate were subjected to Western blotting.

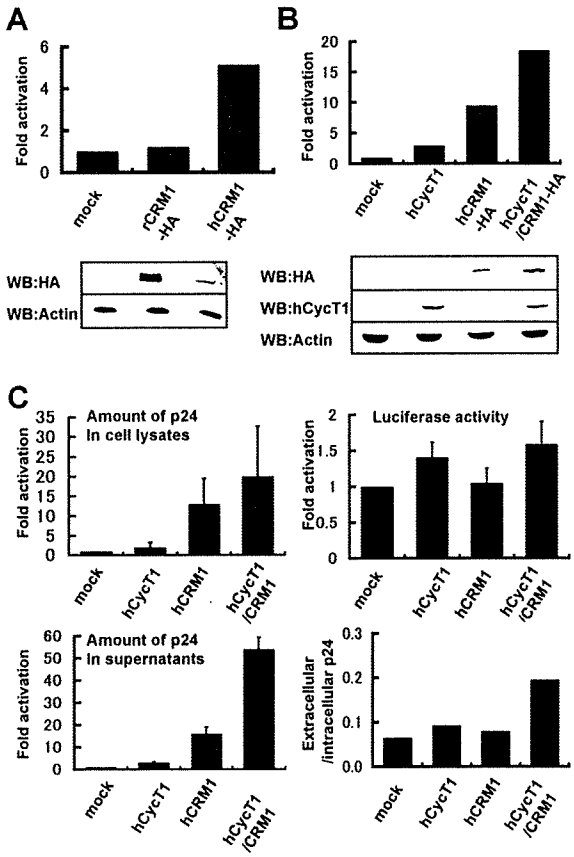

Figure 3
Synergistic effect of hCycT1 and hCRM1 in rat macrophage cell lines. (A) NR8383 cells were electroporated as described in Fig. 1B. The percentage of living cells was approximately 20–40%, and approximately 75% of the living cells were GFP+. The amount of p24 in the sample containing hCRM1-HA was 196 pg. Approximately 50 μg samples of the cell lysates were subjected to Western blotting as described in the Methods. (B) NR8383 cell lines were electroporated as described in Fig. 1A. The percentage of living cells was approximately 15%, and approximately 60% of the living cells were GFP+. The amount of p24 in the sample containing hCRM1-HA/hCycT1 was 56 pg. (C) NR8383 cell lines were electroporated with 2 μg pΔpol, 0.4 μg pH1-Luc and 0.2 μg pCDMβ-gal along with or without 1 μg pβhCycT1 and 0.5 μg pSRαhCRM. pSRα296 was added to adjust the total amount of the plasmids. The amounts of p24 in the cell lysate and medium of the sample containing hCRM1/hCycT1 were 488 and 96 pg, respectively. Values are means of triplicate samples.

by greater than 20–50 fold in NR8383 cells (Fig. 3B and 3C). The amount of extracellular p24 increased more than intracellular p24, as seen in T cells, suggesting that the increase in Gag expression facilitated more efficient release of viral particles. These results clearly indicate that hCRM1 augments p24 production in rat macrophages

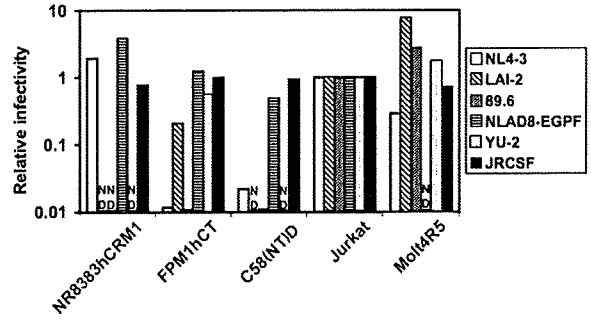

Figure 4
Infectivity of HIV-1 produced in rat and human cells. The medium [containing 50 or 500 pg of p24] from the various cell types electroporated with infectious clones was used to infect TZM-bl cells, and luciferase activity in the TZM-bl cells infected with various progeny viruses was normalized to that in cells infected with HIV-1 released from Jurkat cells. The relative infectivity of HIV-1 from Jurkat cells was normalized to 1. N.D: not determined.

more efficiently than hCycT1, in contrast to the effects of the two proteins in rat T cell lines.

Infectivity of HIV-1 produced by rat cells

To investigate whether HIV-1 produced by rat cells is infectious, we electroporated infectious HIV-1 molecular clones into rat and human cells and evaluated the infectivity of the progeny viruses using the indicator TZM-bl cells, which express luciferase upon HIV infection [26]. Luciferase activity versus inoculated p24 was used as a surrogate marker of infectivity. Interestingly, R5 viruses produced in rat T cells, including the JR-CSF [27], YU-2 [28], and NL-AD8 [29] strains, were equally infectious compared to those produced by human T cells, whereas rat T cell-derived ×4 and dual tropic viruses such as NL4-3 [30], LAI-2 [31], and 89.6 [32] varied in their infectivity. In contrast, both R5 and ×4 viruses produced in the macrophage cell line exhibited infectivities comparable to those from human cells (Fig. 4).

Characterization of hCycT1 and hCRM1 Tg rats

To examine the role of hCycT1 in primary cells, we constructed transgenic (Tg) rats that express hCycT1. Since the regulation of cyclinT1 gene expression is complex [33], a BAC harboring the entire human cyclinT1 gene, which is assumed to contain all the regulatory sequences, was microinjected into fertilized rat eggs. To confirm the expression of hCycT1 in the Tg rats, cells isolated from both thymus and spleen were analyzed by Western blotting using anti-hCycT1. Thymocytes, but not splenocytes, of Tg rats expressed hCycT1 (Fig. 5A). Since hCycT1 is expressed during the activation of human lymphocytes [33], we stimulated the splenocytes with anti-CD3 and anti-CD28. Expression of hCycT1 was detected within 1

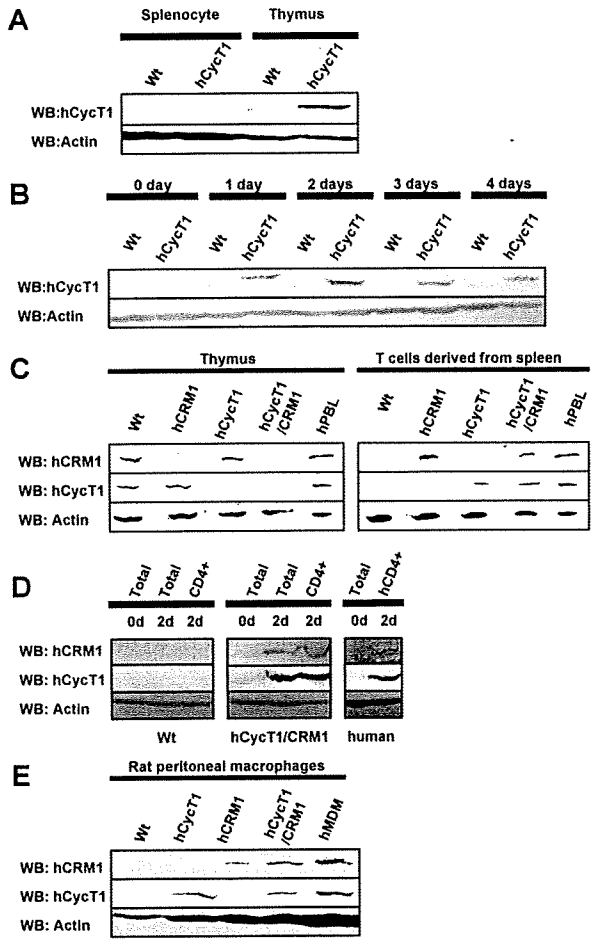

Figure 5
Characterization of hCycT1 and hCRM1 Tg rats. (A) The expression of hCycT1 in spleen- and thymus-derived cells from WT or hCycT1 Tg rats was confirmed by Western blotting using anti-hCycT1. (B) T cells derived from the spleen of WT or hCycT1 Tg rats were stimulated with anti-rat-CD3 and anti-rat-CD28. Cells were collected at the indicated times and subjected to Western blotting using anti-hCycT1. (C) The expression of hCycT1 and hCRM1 in spleen- and thymus-derived cells (C), total T and $CD4^+CD8^-$ T cells (D), and macrophages (E) in WT or Tg rats was confirmed by Western blotting using anti-hCycT1 and anti-hCRM1. T cells derived from the spleen of WT or hCycT1 Tg rats were stimulated with anti-rat-CD3 and anti-rat-CD28.

day and peaked 2 days after stimulation (Fig. 5B). Interestingly, rat splenocytes stimulated with phytohemaglutinin (PHA) and IL-2 did not express hCyCT1 (data not shown).

Expression of hCRM1 in Tg rats was also examined, using a previously established Tg rat [34]. hCRM1 was expressed in both thymocytes and splenocytes activated with anti-CD3/CD28 (Fig. 5C). hCRM1 was not expressed in unstimulated splenocytes (data not shown), consistent with hCRM1 expression in human PBMC [34]. We further characterized total T cells and $CD4^+CD8^-$ T cells prepared from double Tg rats in comparison to rat total T cells and human $CD4^+CD8^-$ T cells 2 days after stimulation. Both hCycT1 and hCRM1 were expressed in activated $CD4^+CD8^-$ T cells prepared from the Tg rat, similar to human $CD4^+CD8^-$ T cells (Fig. 5C and 5D). Both hCycT1 and hCRM1 were expressed in rat peritoneal macrophages at levels equivalent to expression in human monocyte-derived macrophages (MDMs) (Fig. 5E).

Ex vivo p24 production in T cells derived from hCycT1/CRM1 Tg rats

To investigate the effects of hCycT1 and hCRM1 on p24 production in primary T cells, we prepared T cells from splenocytes of wild-type (WT) and Tg rats and stimulated them with anti-CD3/CD28. As a control, isolated human PBLs were activated. In these experiments we used pCRRE [35], which harbors an HIV-1 genome with a deletion in the region from pol to vpr, instead of pΔpol [24], since introducing either pΔpol or the full-sized HIV-1 genome into the primary T cells by any method, including electroporation or VSV-G coated virus, had limited success.

T cells derived from hCycT1 Tg rats produced approximately 10–15 fold more p24 than WT T cells. In T cells derived from hCRM1 Tg rats, p24 production increased approximately 3 fold over WT cells. T cells-derived from hCycT1/CRM1 doubly Tg rats produced p24 at levels 24–40 fold greater than WT, and this level was ~40% of that produced by hPBLs (Fig. 6A). We further examined p24 production by $CD4^+CD8^-$ T cells prepared from double Tg rats in comparison to WT rat and human cells. $CD4^+CD8^-$ T cells prepared from double Tg rats produced p24 in the medium approximately 180 fold more efficiently than WT rat cells; this level was ~11% of the amount of p24 produced by human $CD4^+CD8^-$ T cells (Fig. 6C). These results indicate that the synergistic effects of hCycT1 and hCRM1 promoted the production of p24 in rat primary T cells *ex vivo*.

When intracellular p24 was evaluated by ELISA, increases of approximately 7 and 17 fold were observed in total T and $CD4^+CD8^-$ T cells, respectively (Fig. 6B and 6D), considerably less than the amount of extracellular p24 described above. The ratio of extracellular p24 to intracellular p24 increased gradually as p24 production increased, suggesting a more efficient virus release from the double Tg rat T cells compared to WT rat T cells.

Ex vivo p24 production in peritoneal macrophages derived from hCycT1/CRM1 Tg rats

To investigate HIV-1 propagation in macrophages derived from Tg rats, we prepared $CD11b^+ED2^+$ peritoneal macro-

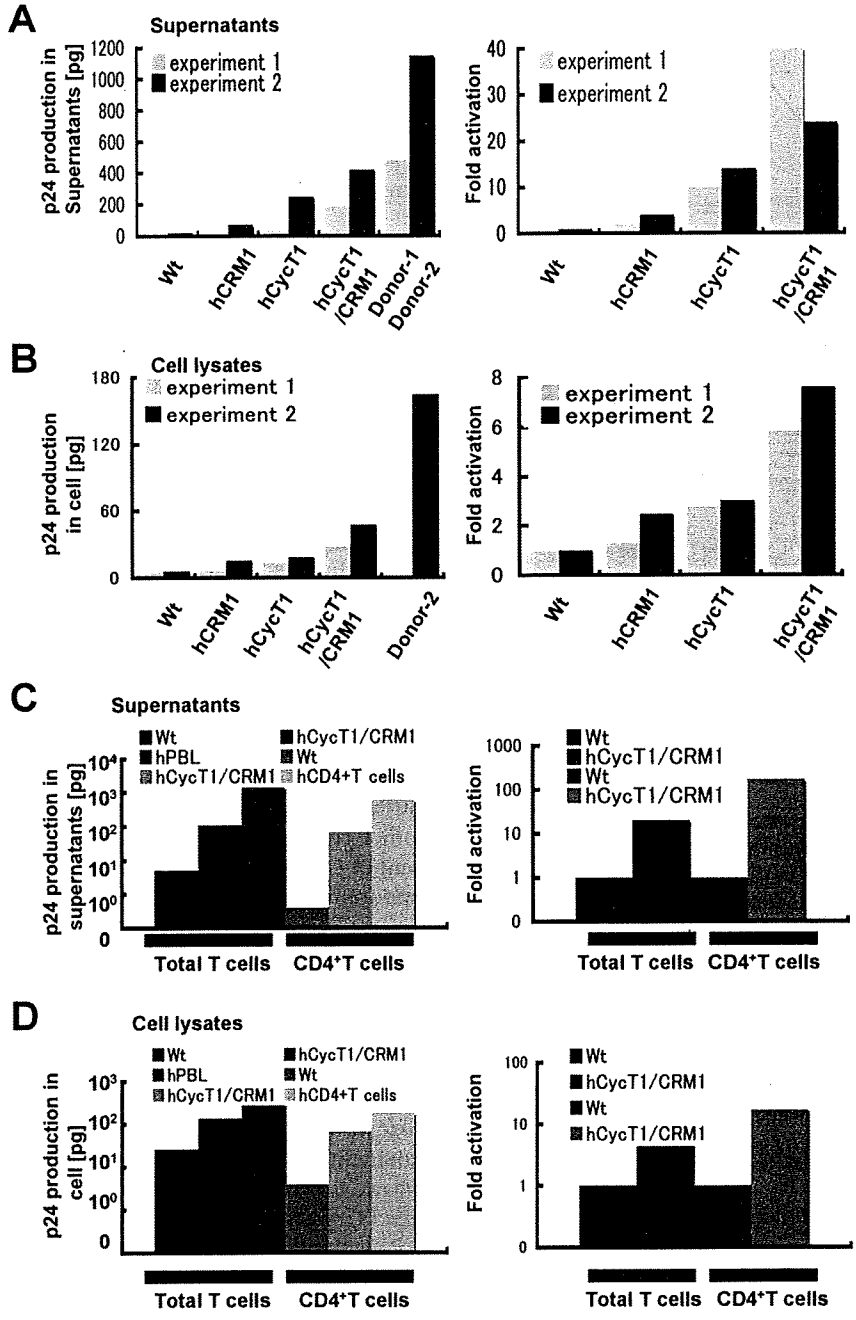

Figure 6

Quantification of p24 production in the total T cell fraction and CD4$^+$CD8$^-$ T cell fraction derived from hCycT1/CRM1 Tg rats. Stimulated spleen-derived T cells from WT or Tg rats and hPBL were electroporated with 4 μg PCRRE and 1 μg pMax-GFP, and p24 production in the supernatants (A) and cell lysates (B) was measured by ELISA (left panel). The percentage of living cells was 30–40%, and 28–40% of the living cells were GFP$^+$. The right panels represent the fold activation of Tg versus WT rats. Stimulated CD4$^+$CD8$^-$ T cells derived from WT, hCycT1/CRM1 Tg rats, and human blood were electroporated, as above, and p24 production in the supernatants (C) and cell lysates (D) was measured. The percentage of living cells was ~10%, and 30–40% of the living cells were GFP$^+$. Values are the means of duplicate samples.

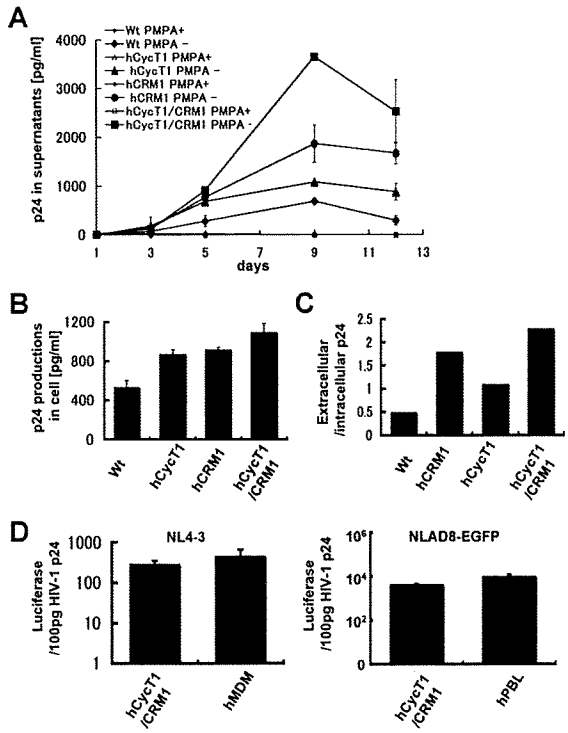

Figure 7
Quantification of p24 production in rat peritoneal macrophages. (A) Rat peritoneal macrophages or human MDMs were infected with VSV-G pseudotyped NL4-3 virus. The amount of p24 in the medium was then measured by ELISA. (B) The infected cells were harvested 12 days after infection and intracellular p24 levels were evaluated. (C) The ratio of the amount of extracellular to intracellular p24 was calculated. (D) Infectivity of viruses present in the medium 5 days after infection was measured using TZM-bl cells. NLAD8-EGFP was used to infect 5 × 10^5 macrophages from double Tg rats or human PBL, and the medium was recovered 5 days after infection. Values are the means of triplicate samples.

phages and subsequently infected the cells using HIV-1 pseudotyped with VSV G protein. Although WT peritoneal macrophages produced a considerable amount of HIV-1 progeny virus in the absence of hCRM1 and hCycT1 expression, macrophages derived from hCycT1/CRM1 doubly Tg rats produced 6 fold higher levels of p24 at their peak (Fig. 7A). This level corresponds to 20% of the amount of p24 produced by human MDMs (data not shown). Macrophages from hCRM1 Tg rats supported a several fold increase in p24 production, but hCycT1 expression had a smaller effect. Macrophages treated with PMPA, a reverse transcriptase inhibitor, did not produce significant amounts of p24, confirming that the p24 measured represents production of progeny viruses and not inoculum. The amount of intracellular p24 also increased to some extent in the Tg rats, but to a lesser extent than p24 levels in the medium (Fig. 7B). Approximately 67% of the p24 synthesized in the doubly Tg cells was released into the medium and the ratio of extracellular p24 to intracellular p24 increased as viral production increased (Fig. 7C).

The infectivity of the viruses, which were harvested 5 days post infection, was evaluated using TZM-bl cells. Figure 7D shows that both R5 and ×4 viruses produced from rat macrophages retained infectivity levels similar to those from human PBLs and MDMs.

Discussion

In the present study, we demonstrated the effects of hCycT1 and hCRM1 on augmentation of HIV-1 Gag production in both established and primary rat T cells and macrophages. hCycT1 enhanced p24 production profoundly in rat T cells, suggesting that hCycT1 is an essential gene that should be included in the construction of a rat model of HIV-1 infection. Although our results are in contrast to the previous reports of only a 2–5 fold increase in early gene expression in rat primary T cells and epithelial cells expressing hCycT1 [7,10,16,17], the overall effects stemmed from the increased HIV-1 pre-mRNA in response to hCycT1 expression included an increase in Tat/Rev proteins and enhanced efficiency of p24 release from T cells. This may explain the remarkable enhancement of p24 levels in the extracellular milieu. Our results support and extend the effect of hCycT1 expressed in rat primary T cells originally described by Michel et al [17]. In contrast, hCycT1 expression in macrophages had only a minor effect on p24 production. Since the level of LTR-driven luciferase activity in NR8383 cells in the absence of hCycT1 was similar to Molt4 cells (data not shown), the high basal activity of LTR-driven gene expression may explain the diminished effect of hCycT1 expression. These data are consistent with the relatively high HIV-1 LTR activity in primary macrophages [7,16,17]. Since rCycT1, like mCycT1, has a tyrosine at residue 261 in place of the hCycT1 cysteine [7], which is crucial for binding to the TAR element, rCycT1 itself may not be functional in LTR-driven expression. Instead, rat epithelial cells and macrophages may support transcription in a Tat independent manner. Alternatively, other factors in these cells may cooperate with rCycT1 for efficient LTR-driven expression.

The expression of hCRM1 in the rat macrophage line NR8383 profoundly augmented the production of p24, suggesting that Rev function is impaired and that inclusion of the hCRM1 gene in construction of a rat model for HIV-1 infection should be considered. Moreover, the profound effects of hCRM1 expression have been observed in several rat epithelial cell lines (data not shown); rCRM1

may support Rev function less efficiently. However, the effect of hCRM1 was not as great in T cell lines, primary T cells, or macrophages, compared to the macrophage cell line. These observations suggest that CRM1 function may be affected by factors involved in the formation of gag mRNA, such as the cell type-specific efficiency of splicing.

In mouse cells, defects in HIV particle formation and release have been reported [11] due to incorrect transport of gag mRNA from the nucleus to the cytoplasm [36]. The release of viral particles from both primary rat T cells and macrophages was inefficient when p24 production was low. However, when p24 production was enhanced by expression of hCycT1 in T cells or hCRM1/hCycT1 in macrophages, p24 was released more efficiently. These results suggest that the intracellular concentration of Gag protein is critical for efficient virus formation. However, rat tetherin, which is resistant to Vpu-induced degradation, may reduce the release of viral particles, although this effect was demonstrated using tetherin overexpression [37]. Since we observed that the efficiency of viral release was variable under different conditions (compare panels of Fig. 6), the inhibitory effect of rat tetherin may be an important subject for future study.

Both R5 and ×4 viruses produced from rat macrophages are as infectious as those produced by human macrophages, consistent with the report of Keppler et al. [8]. In contrast, ×4 and dual-tropic viruses that were produced in rat T cells had varying infectivities, although several R5 strains produced in rat T cells were as infectious as human T cell-produced viruses. These differences in infectivity may be ascribed to the envelope because the AD8 strain was constructed by substituting M-tropic *env* for the counterpart *env* fragment in pNL4-3 [29]. Investigating the causes of these differences in infectivity will enable us to make a rat model that allows for propagation of various strains of HIV-1.

The efficiency of the early steps of infection, including reverse transcription, nuclear import, and integration in macrophages and T cells of Sprague-Dawley rats is comparable to human cells, in contrast to the low rate of integration in mouse T cells [8,16,38]. We have also efficiently infected rat macrophages using VSV-G-coated viruses. However, the very low rate of infection of primary T cells from the rat F344 strain used in this study has hampered our detailed analysis, and suggested that inhibitory factors affecting viral penetration, similar to monkey Trim5α [39], may be present. Further studies on the mode of HIV infection in each rat strain will be required.

Conclusion

Expression of both hCycT1 and hCRM1 synergistically enhanced p24 production in rat T cells and macrophages to levels approximately 10–40% of those detected in human cells. R5 viruses produced in the rat cells were infectious. Moreover, the efficiency of the early steps of HIV-1 infection in some rat cells has been reported to be comparable to human cells [8,16]. Collectively, these results suggest that rats that express human CD4, CCR5, CycT1, and CRM1 may provide the basis for a good model system that supports multiple cycles of HIV-1 infection.

Competing interests

The authors declare that they have no competing interests.

Authors' contributions

HS and TO designed the study. HO conducted the majority of the experiments. XZ performed and analyzed infection experiments. IBF and HS constructed and maintained the transgenic rats. MN constructed HA-tagged CRM1 plasmids. HS and HO wrote the paper. All authors approved the final manuscript.

Acknowledgements

We thank A. Hirano and N. Mizuno for technical assistance. PMPA, pH1-luc, pΔpol, pβCycT, pYK-JRCSF, pNLAD8-EGFP, and pSRαhCRM1-HA were kind gifts from Dr. E. DeClercq (Reg Institute for Medical Research), Dr. A. Adachi (Tokushima University), Dr. Y. Iwakura (Tokyo University), Dr. Y. Koyanagi (Kyoto University), Dr. K. T. Jeang (George Washington University), and Dr. T. Kimura (Ritumeikan University), respectively. Human blood was the kind gift of the Hokkaido Red Cross Blood Center (Sapporo, Japan). The infectious molecular HIV-1 clones and TZM-bl cells were obtained through the AIDS Research and Reference Reagent program. This study was supported by grants from the Ministry of Sports and Culture (Japan), and the Ministry of Health and Welfare (Japan).

References

1. Giuffre AC, Higgins J, Buckheit RW, North TW: **Susceptibilities of simian immunodeficiency virus to protease inhibitors.** *Antimicrob Agents Chemother* 2003, **47**:1756-1759.
2. Hazuda DJ, Young SD, Guare JP, Anthony NJ, Gomez RP, Wai JS, Vacca JP, Handt L, Motzel SL, Klein HJ, Dornadula G, Danovich RM, Witmer MV, Wilson KA, Tussey L, Schleif WA, Gabryelski LS, Jin L, Miller MD, Casimiro DR, Emini EA, Shiver JW: **Integrase inhibitors and cellular immunity suppress retroviral replication in rhesus macaques.** *Science* 2004, **305**:528-532.
3. Hu SL: **Non-human primate models for AIDS vaccine research.** *Curr Drug Targets Infect Disord* 2005, **5**:193-201.
4. Veazey RS, Klasse PJ, Schader SM, Hu Q, Ketas TJ, Lu M, Marx PJ, Dufour J, Colonno RJ, Shattock RJ, Springer MS, Moore JP: **Protection of macaques from vaginal SHIV challenge by vaginally delivered inhibitors of virus-cell fusion.** *Nature* 2005, **438**:99-102.
5. Shultz LD, Ishikawa F, Greiner DL: **Humanized mice in translational biomedical research.** *Nat Rev Immunol* 2007, **7**:118-130.
6. Watanabe S, Terashima K, Ohta S, Horibata S, Yajima M, Shiozawa Y, Dewan MZ, Yu Z, Ito M, Morio T, Shimizu N, Honda M, Yamamoto N: **Hematopoietic stem cell-engrafted NOD/SCID/IL2R gamma null mice develop human lymphoid systems and induce long-lasting HIV-1 infection with specific humoral immune responses.** *Blood* 2007, **109**:212-218.
7. Keppler OT, Yonemoto W, Welte FJ, Patton KS, Iacovides D, Atchison RE, Ngo T, Hirschberg DL, Speck RF, Goldsmith MA: **Susceptibility of rat-derived cells to replication by human immunodeficiency virus type 1.** *J Virol* 2001, **75**:8063-8073.
8. Keppler OT, Welte FJ, Ngo TA, Chin PS, Patton KS, Tsou CL, Abbey NW, Sharkey ME, Grant RM, You Y, Scarborough JD, Ellmeier W, Littman DR, Stevenson M, Charo IF, Herndier BG, Speck RF, Gold-

smith MA: **Progress toward a human CD4/CCR5 transgenic rat model for de novo infection by human immunodeficiency virus type 1.** *J Exp Med* 2002, **195**:719-736.
9. Browning J, Horner JW, Mantovani MP, Raker C, Yurasov S, DePinho RA, Goldstein H: **Mice transgenic for human CD4 and CCR5 are susceptible to HIV infection.** *Proc Natl Acad Sci USA* 1997, **94**:14637-14641.
10. Bieniasz PD, Cullen BR: **Multiple blocks to human immunodeficiency virus type 1 replication in rodent cells.** *J Virol* 2000, **74**:9868-9877.
11. Mariani R, Rasala BA, Rutter G, Wiegers K, Brandt SM, Kräusslich HG, Landau NR: **A Block to Human Immunodeficiency Virus Type 1 Assembly in Murine Cells.** *J Virol* 2000, **74**:3859-3870.
12. Wei P, Garber ME, Fang SM, Fischer WH, Jones KA: **A novel CDK9-associated C-type cyclin interacts directly with HIV-1 Tat and mediates its high affinity, loop-specific binding to TAR RNA.** *Cell* 1998, **92**:451-462.
13. Bieniasz PD, Grdina TH, Bogerd HP, Cullen BR: **Recruitment of a protein complex containing Tat and cyclin T1 to TAR governs the species specificity of HIV-1 Tat.** *EMBO J* 1998, **17**:7056-7065.
14. Garber ME, Wei P, KewalRamani VN, Mayall TP, Herrmann CH, Rice AP, Littman DR, Jones KA: **The interaction between HIV-1 Tat and human cyclin T1 requires zinc and a critical cysteine residue that is not conserved in the murine CycT1 protein.** *Genes Dev* 1998, **15**:3512-3527.
15. Sun J, Soos T, Kewalramani VN, Osiecki K, Zheng JH, Falkin L, Santambrogio L, Littman DR, Goldstein H: **CD4-Specific Transgenic Expression of Human Cyclin T1 Markedly Increases Human Immunodeficiency Virus Type 1 (HIV-1) Production by CD4 T Lymphocytes and Myeloid Cells in Mice Transgenic for a Provirus Encoding a Monocyte-Tropic HIV-1 Isolate.** *J Virol* 2006, **80**:1850-1862.
16. Goffinet C, Michel N, Allespach I, Tervo HM, Hermann V, Krausslich HG, Greene WC, Keppler OT: **Primary T-cells from human CD4/CCR5-transgenic rats support all early steps of HIV-1 replication including integration, but display impaired viral gene expression.** *Retrovirology* 2007, **4**:53-68.
17. Michel N, Goffinet C, Ganter K, Allespach I, KewalRmani VN, Saifuddin M, Littman DR, Greene WC, Goldsmith MA, Keppler OT: **Human cyclin T1 expression ameliorates a T-cell-specific transcriptional limitation for HIV in transgenic rats, but is not sufficient for a spreading infection of prototypic R5 HIV-1 strains ex vivo.** *Retrovirology* 2009, **6**:2-18.
18. Koito A, Shigekane H, Matsushita S: **Ability of small animal cells to support the postintegration phase of human immunodeficiency virus type-1 replication.** *Virology* 2003, **305**:181-191.
19. Nekhai S, Jeang KT: **Transcriptional and post-transcriptional regulation of HIV-1 gene expression: role of cellular factors for Tat and Rev.** *Future Microbiol* 2006, **1**:417-426.
20. Fornerod M, Ohno M, Yoshida M, Mattaj IW: **CRM1 is an export receptor for leucine-rich nuclear export signals.** *Cell* 1997, **90**:1051-1060.
21. Fukuda M, Asano S, Nakamura T, Adachi M, Yoshida M, Yanagida M, Nishida E: **CRM1 is responsible for intracellular transport mediated by the nuclear export signal.** *Nature* 1997, **390**:308-311.
22. Malim MH, McCarn DF, Tiley LS, Cullen BR: **Mutational definition of the human immunodeficiency virus type 1 Rev activation domain.** *J Virol* 1991, **65**:4248-4254.
23. Zheng YH, Yu HF, Peterlin BM: **Human p32 protein relieves a posttranscriptional block to HIV replication in murine cells.** *Nat Cell Biol* 2003, **5**:611-618.
24. Iwakura Y, Shioda T, Tosu M, Yoshida E, Hayashi M, Nagata T, Shibuta H: **The induction of cataracts by HIV-1 in transgenic mice.** *AIDS* 1992, **6**:1069-1075.
25. Koya Y, Ohashi T, Kato H, Hanabuchi S, Tsukahara T, Takemura F, Etoh K, Matsuoka K, Fujii M, Kannagi M: **Establishment of a seronegative human T-cell leukemia virus type 1 (HTLV-1) carrier state in rats inoculated with a syngeneic HTLV-1-immortalized T-cell line preferentially expressing Tax.** *J Virol* 1999, **73**:6436-6443.
26. Derdeyn CA, Decker JM, Sfakianos JN, Wu X, O'Brien WA, Ratner L, Kappes JC, Shaw GM, Hunter E: **Sensitivity of human immunodeficiency virus type 1 to the fusion inhibitor T-20 is modulated by coreceptor specificity defined by the V3 loop of gp120.** *J Virol* 2000, **74**:8358-8367.
27. Koyanagi Y, Miles S, Mitsuyasu RT, Merrill JE, Vinters HV, Chen IS: **Dual infection of the central nervous system by AIDS viruses with distinct cellular tropisms.** *Science* 1987, **236**:819-822.
28. Li Y, Hui H, Burgess CJ, Price RW, Sharp PM, Hahn BH, Shaw GM: **Complete nucleotide sequence, genome organization, and biological properties of human immunodeficiency virus type 1 in vivo: evidence for limited defectiveness and complementation.** *J Virol* 1992, **66**:6587-600.
29. Rich EA, Orenstein JM, Jeang KA: **A Macrophage-Tropic HIV-1 That Expresses Green Fluorescent Protein and Infects Alveolar and Blood Monocyte- Derived Macrophages.** *J Biomed Sci* 2002, **9**:721-726.
30. Adachi A, Koenig S, Gendelman HE, Daugherty D, Celli SG, Fauci AS, Martin MA: **Productive, persistent infection of human colorectal cell lines with human immunodeficiency virus.** *J Virol* 1987, **61**:209-213.
31. Peden K, Emerman M, Montagnier L: **Changes in growth properties on passage in tissue culture of viruses derived from infectious molecular clones of HIV-1LAI, HIV-1MAL, and HIV-1ELI.** *Virology* 1991, **185**:661-672.
32. Collman R, Balliet JW, Gregory SA, Friedman H, Kolson DL, Nathanson N, Srinivasan A: **An infectious molecular clone of an unusual macrophagetropic and highly cytopathic strain of human immunodeficiency virus type 1.** *J Virol* 1992, **66**:7517-7521.
33. Herrmann CH, Carroll RG, Wei P, Jones KA, Rice AP: **Tat-associated kinase, TAK, activity is regulated by distinct mechanisms in peripheral blood lymphocytes and promonocytic cell lines.** *J Virol* 1998, **72**:9881-9888.
34. Takayanagi R, Ohashi T, Yamashita E, Kurosaki Y, Tanaka K, Hakata Y, Komoda Y, Ikeda S, Yokota T, Tanaka Y, Shida H: **Enhanced replication of human T-cell leukemia virus type 1 in T cells from transgenic rats expressing human CRM1 that is regulated in a natural manner.** *J Virol* 2007, **81**:5908-5918.
35. Kimura T, Hashimoto I, Nishikawa M, Fujisawa JI: **A role for Rev in the association of HIV-1 gag mRNA with cytoskeletal beta-actin and viral protein expression.** *Biochimie* 1996, **78**:1075-1080.
36. Swanson CM, Puffer BA, Ahmad KM, Doms RW, Malim MH: **Retroviral mRNA nuclear export elements regulate protein function and virion assembly.** *EMBO J* 2004, **23**:2632-2640.
37. Goffinet C, Allespach I, Homann S, Tervo HM, Habermann A, Rupp D, Oberbremer L, Kern C, Tibroni N, Welsch S, Locker JK, Banting G, Kräusslich HG, Fackler OT, Keppler OT: **HIV-1 Antagonism of CD317 is species specific and involves Vpu-mediated proteasomal degradation of the Restriction Factor.** *Cell Host & Microbe* 2009, **5**:285-297.
38. Tervo HM, Goffinet C, Keppler OT: **Mouse T-cells restrict replication of human immunodeficiency virus at the level of integration.** *Retrovirology* 2008, **5**:58-73.
39. Stremlau M, Owens CM, Perron MH, Kiessling M, Autissier P, Sodroski J: **The cytoplasmic body component TRIM5alpha restricts HIV-1 infection in Old World monkeys.** *Nature* 2004, **427**:848-853.
40. Zhang X, Hakata Y, Tanaka Y, Shida H: **CRM1, an RNA transporter, is a major species-specific restriction factor of human T cell leukemia virus type 1(HTLV-1) in rat cells.** *Microbes Infect* 2006, **8**:851-859.
41. Niwa H, Yamamura K, Miyazaki J: **Efficient selection for high expression transfectants with a novel eukaryotic vector.** *Gene* 1991, **108**:193-199.
42. Takebe Y, Seiki M, Fujisawa J, Hoy P, Yokota K, Arai K, Yoshida M, Arai N: **SR alpha promoter: an efficient and versatile mammalian cDNA expression system composed of the simian virus 40 early promoter and the R-U5 segment of human T-cell leukemia virus type 1 long terminal repeat.** *Mol Cell Biol* 1988, **8**:466-472.
43. Hakata Y, Yamada M, Shida H: **Rat CRM1 is responsible for the poor activity of human T-cell leukemia virus type 1 Rex protein in rat cells.** *J Virol* 2001, **75**:11515-11525.
44. Tsai CC, Follis KE, Sabo A, Beck TW, Grant RF, Bischofberger N, Benveniste RE, Black R: **Prevention of SIV Infection in Macaques by (R)-9-(2-Phosphonylmethoxypropyl) adenine.** *Science* 1995, **270**:1197-1199.

Cellular Immunology 259 (2009) 165–176

Contents lists available at ScienceDirect

Cellular Immunology

journal homepage: www.elsevier.com/locate/ycimm

Preliminary *in vivo* efficacy studies of a recombinant rhesus anti-$\alpha_4\beta_7$ monoclonal antibody ☆

L.E. Pereira [a], N. Onlamoon [a], X. Wang [b], R. Wang [b], J. Li [b], K.A. Reimann [b], F. Villinger [a], K. Pattanapanyasat [c], K. Mori [d], A.A. Ansari [a,*]

[a] Department of Pathology & Laboratory Medicine, Emory University School of Medicine, Room 2309 WMB, 101 Woodruff Circle, Atlanta, GA 30322, USA
[b] Division of Viral Pathogenesis, Beth Israel Deaconess Medical Center, 330 Brookline Avenue, Boston, MA 02215, USA
[c] Office for Research and Development, Department of Immunology, Faculty of Medicine, Siriraj Hospital, Mahidol University, Bangkok, Thailand
[d] AIDS Research Center, National Institute of Infectious Diseases, Tokyo 162-8640, Japan

ARTICLE INFO

Article history:
Received 30 April 2009
Accepted 10 June 2009
Available online 26 June 2009

Keywords:
Cell trafficking
Antibodies
AIDS
T-cells
Rhesus macaque
Act1
Alpha4beta7 integrin

ABSTRACT

Recent findings established that primary targets of HIV/SIV are lymphoid cells within the gastrointestinal (GI) tract. Focus has therefore shifted to T-cells expressing $\alpha_4\beta_7$ integrin which facilitates trafficking to the GI tract via binding to MAdCAM-1. Approaches to better understand the role of $\alpha_4\beta_7$+ T-cells in HIV/SIV pathogenesis include their depletion or blockade of their synthesis, binding and/or homing capabilities *in vivo*. Such studies can ideally be conducted in rhesus macaques (RM), the non-human primate model of AIDS. Characterization of $\alpha_4\beta_7$ expression on cell lineages in RM blood and GI tissues reveal low densities of expression by NK cells, B-cells, naïve and TEM (effector memory) T-cells. High densities were observed on TCM (central memory) T-cells. Intravenous administration of a single 50 mg/kg dose of recombinant rhesus $\alpha_4\beta_7$ antibody resulted in significant initial decline of $\alpha_4\beta_7$+ lymphocytes and sustained coating of the $\alpha_4\beta_7$ receptor in both the periphery and GI tissues.

1. Introduction

It is now established that the gut-associated lymphoid tissue (GALT) is the major initial target of pathology during acute infection of humans with HIV-1 or rhesus macaques (RM) with SIV [1–9]. During this period of primary infection, a significant frequency of CD4+ memory T-cells, which are CCR5+ and already in a state of activation due in part to exposure and response to intestinal flora, serve as prime targets for the virus leading to their infection and subsequent depletion via direct cytopathic effects and/or indirect mechanisms of apoptosis. The degree of impact of this major localized effect has been hypothesized to significantly influence the course of disease and has therefore led to a more detailed study of the mechanisms associated with T-cells that migrate and/or reside within the gastrointestinal tract. The intestinal homing receptors CCR9 and $\alpha_4\beta_7$ play one of the central roles in promoting the migration of lymphocytes into intestinal mucosal tissue via binding to CCL25 and mucosal addressin cell adhesion molecule-1 (MAdCAM), respectively [10–15]. The $\alpha_4\beta_7$ cell surface receptor has received much attention particularly in light of a recent study by Arthos et al. which demonstrated that the HIV-1 envelope protein gp120 binds to an active form of $\alpha_4\beta_7$ on CD4+ T-cells and initiates LFA-1 activation that facilitates formation of a viral synapse leading to cell-to cell spreading further facilitating viral infection [16]. Thus, the ability of the host to defend itself against lentiviral infection is likely to depend on the nature (such as phenotype and frequency) of these gut-homing lymphocytes. For instance, gut-homing virus-specific NK cells and CD8+ CTLs may contribute to the containment of HIV/SIV viral replication while gut-homing CD4+ T-cells besides their expected T helper cell activity may simply provide additional targets for the virus and sustain its replication. A detailed understanding of the immune responses in mucosal sites particularly during early stages of infection is therefore critical and because there is increasing evidence to support a significant contributing role for $\alpha_4\beta_7$+ cells in HIV pathogenesis, it is important to fully understand the part played by these cells in early viral infection and subsequent disease progression. One approach that can be taken to accomplish this aim is by conducting *in vivo* studies that utilize an anti-$\alpha_4\beta_7$ monoclonal antibody to either block $\alpha_4\beta_7$ receptor and trafficking or to deplete $\alpha_4\beta_7$+ cells prior to or during acute viral infection. This can best be studied in RM recognized to be the optimal non-human primate model for the study of AIDS. When infected with SIV, this species exhibits CD4+ T-cell depletion,

☆ Supported by NIH RO1 AI 078773-01, NOI AI 040101, R24 RR016001, grants from the Thailand Research Fund and the Ministry of Health, Labor and Welfare, Japan.

* Corresponding author.
E-mail address: pathaaa@emory.edu (A.A. Ansari).

0008-8749/$ - see front matter © 2009 Elsevier Inc. All rights reserved.
doi:10.1016/j.cellimm.2009.06.012

chronic immune activation, immune exhaustion and disease remarkably similar to HIV infection in humans [17–24]. Furthermore, the GI pathology observed in acutely HIV-infected patients is similar to the pathology exhibited by SIV-infected RM [3,7–9,25]. However, while the expression of $\alpha_4\beta_7$ on major cell lineages in humans has been documented, there is a paucity of data with regards to $\alpha_4\beta_7$-expressing cells and the effect of SIV infection on this gut-homing marker in RM. In humans, flow cytometry utilizing Act I, a murine monoclonal antibody specific for human $\alpha_4\beta_7$ integrin (henceforth referred to as murine $\alpha_4\beta_7$ mAb), showed expression of both low and high density $\alpha_4\beta_7$ ($\alpha_4\beta_7^{low}$ and $\alpha_4\beta_7^{high}$) on adult T-cells and B-cells while NK cells, eosinophils, and neonatal T- and B-cells exhibited a $\alpha_4\beta_7^{low}$ pattern of expression [10,12,26]. Furthermore, while $\alpha_4\beta_7^{low}$ was expressed by naïve T- and B-cells, $\alpha_4\beta_7^{high}$ was observed on memory T- and B-cells. Cell subsets with an $\alpha_4\beta_7^{high}$ phenotype are believed to express this receptor in an active form and are thought to be those that preferentially migrate to and following binding to their cognate MAdCAM ligand, reside within the GI tract. Several studies primarily conducted utilizing murine models have shown that the induction of $\alpha_4\beta_7^{high}$ expression on T-cells is attributed to retinoic acid (RA), which is a vitamin A metabolite catabolized specifically by either mucosal dendritic and/or stromal cells [11,15,27–32].

Thus, it was reasoned that baseline studies on the cell lineages that express $\alpha_4\beta_7$ in tissues from RM would be a pre-requisite prior to pursuing *in vivo* $\alpha_4\beta_7$+ cell-depleting and/or blocking studies in SIV-infected macaques. The purpose of the current study was therefore twofold; first, to characterize and compare $\alpha_4\beta_7$ expression levels on the major cell lineages involved in innate and adaptive immunity from healthy uninfected RM by multi-parameter flow cytometry and to evaluate the *in vitro* and *in vivo* effects of RA and SIV infection, respectively, on $\alpha_4\beta_7$ induction and/or mobilization of $\alpha_4\beta_7$+ lymphocyte subsets. Second, after acquiring a sound understanding of these factors, to conduct a preliminary safety and efficacy study of the *in vivo* administration of a monoclonal rhesus $\alpha_4\beta_7$+ antibody in RM. The results of our studies show a differential pattern of $\alpha_4\beta_7$ expression among the major cell lineages and their subsets which is similar to what has been reported for human lymphocytes. *In vitro* incubation with RA was also found to significantly induce $\alpha_4\beta_7$ expression on activated T-cells. Furthermore, while significant decreases in the frequency of $\alpha_4\beta_7$+ lymphocytes were noted in rectal biopsy tissues, no significant changes in the frequency of $\alpha_4\beta_7$+ cells were noted in the periphery of chronically SIV-infected RM. Of interest was the finding that there was a rapid disappearance of select subsets of $\alpha_4\beta_7$+ NK and $\alpha_4\beta_7$+ CD4+ T-cells in the periphery during the acute infection period. Finally, a preliminary study was conducted to define the potential *in vivo* depletion and/or blocking activity of a novel $\alpha_4\beta_7$ monoclonal antibody (modified to create a less immunogenic rhesus recombinant construct Rh-$\alpha_4\beta_7$) which was administered intravenously as a single bolus dose to healthy RM. The infusion of a single dose (50 mg/kg) of Rh-$\alpha_4\beta_7$ mAb was found to be non-toxic and lead to an initial significant decline followed by a failure to detect (up to 5 weeks) $\alpha_4\beta_7$+ lymphocytes in both peripheral and GI compartments. Collectively these data provides the foundation for *in vitro* and *in vivo* manipulation of $\alpha_4\beta_7$+ lymphocytes for potential mechanistic-based experiments in SIV-infected animals. The implications of these current findings for future studies are discussed.

2. Materials and methods

2.1. Animals

Healthy uninfected and SIV-infected RM were housed at the Yerkes National Primate Research Center (YNPRC) of Emory University. Their housing, care, diet and maintenance was in conformance to the guidelines of the Committee on the Care and Use of Laboratory Animals of the Institute of Laboratory Animal Resources, National Research Council and the Health and Human Services guidelines "Guide for the Care and Use of Laboratory Animals." The RM involved in the cross-sectional and longitudinal study were infected intravenously with 200 TCID50 of SIVmac239. All uninfected and SIV-infected RM used in the study were male and age matched adults.

2.2. Specimen collection and blood processing

Peripheral blood mononuclear cells (PBMC) were isolated by standard Ficoll–Hypaque gradient centrifugation from heparinized whole blood. This procedure in addition to those for specimen collection of and lymphocyte isolation from colon, jejunum tissues, rectal biopsies and bronchial alveolar lavage (BAL) were performed as described previously [33–35].

2.3. Viral load determination

Plasma viral loads were determined using a competitive reverse transcriptase polymerase chain reaction assay by the Virology Core Lab supported by the Emory University CFAR. To determine if the $\alpha_4\beta_7$ subset of CD4+ T-cells were preferentially infected with SIV, PBMC were isolated from the peripheral blood of 6 SIV-infected rhesus macaques during the chronic stage of infection. All monkeys were asymptomatic at the time of blood sampling. We selected three monkeys that had high (>100,000 copies/ml) and three monkeys that had low plasma viral loads (<10,000 viral copies/ml) to determine the potential role of plasma viral load on cellular viral loads in the CD4+ T-cell subsets. CD4+ T-cells were first enriched by depleting all cell lineages except CD4+ T-cells using a cocktail of monoclonal antibodies. This was followed by incubating the remaining enriched population of CD4+ T-cells with murine $\alpha_4\beta_7$ mAb at 5 μg/ml per million cells at 4 °C for 30 min. The cells were then washed and resuspended in PBS and incubated with anti-mouse Ig conjugated immuno-beads following concentrations as recommended by the commercial vendor. The enriched population of CD4+ $\alpha_4\beta_7$+ and the remaining CD4+ $\alpha_4\beta_7$− cells were then used to determine the levels of SIV. An aliquot of the CD4+ $\alpha_4\beta_7$− isolated population was subjected to flow cytometric analysis to determine degree of purity and found to contain >92% CD4+ and <0.01% $\alpha_4\beta_7$+ cells. RNA was isolated from two million cells from each of the subsets from each of the monkeys using GuHCl/Proteinase K viral lysis solution and guanidium thiocyanate carrier solution. Viral RNA was eluted in 20 μl RNAse free water and stored at −80 °C until use. Viral RNA from all the samples was then individually reverse transcribed using enhanced avian RT first strand synthesis kit and RNAse free oligoprimers (SIVgagrt). Level of viral copies were quantified in each of the cDNA sample using real time PCR using SYBR greenER for iCycler kit and the following RNAse free primer pairs:

SIV gagrt F: TTA TGG TGT ACC AGC TTG GAG GAA TGC

SIV gagrt R: CCA AAC CAA GTA GAA GTC TGT GTC TGT TCC ATC

The sensitivity of the assay was determined to be 10 viral copies/ml.

2.4. Flow cytometry

Multiple clones of monoclonal antibodies with specificity for human CD3, CD8alpha, CD8beta, CD95, CD28, alpha4 integrin (CD49d), beta7 integrin, CD16, CD14, CD20, CD56, and NKG2A, were first screened to identify those that provided optimal cross-reactivity for the identification of various T-cell, B-cell and NK cell lineages and subsets of cells from RM as described previously [33–35]. Our in-house purified and biotinylated murine $\alpha_4\beta_7$ mAb was

incubated with cells for 15 min followed by 10 min staining with PE-Cy7 or APC conjugated streptavidin for the determination of the frequency and absolute numbers of $\alpha_4\beta_7$+ lymphocytes. Stained cells fixed with 1% paraformaldehyde were analyzed on either a FACS Calibur or a LSRII flow cytometer (BD Biosciences, San Jose CA). Flow cytometric acquisition and analysis of samples as well as the gating strategy for identifying total NK cells and its subsets, the CD4+ and CD8+ T-cells subsets in lymphoid cells from rhesus macaques has been described previously [33,34].

2.5. In vitro effects of Retinoic acid (RA) on $\alpha_4\beta_7$expression

PBMC or isolated CD4+ T-cells purified by magnetic beads (Dynal Invitrogen) were cultured in RPMI 1640 media containing antibiotics and 10% fetal calf serum (heretofore referred to as media). Aliquots of such cells were cultured in media containing anti-CD3/CD28 antibody-conjugated magnetic beads [35] and/or 50 U IL-2 for 5 days at 37 °C, 5% CO_2 in the presence or absence of 10 nM all-trans RA (Sigma–Aldrich). The cells were then washed and analyzed for the frequency and relative density of $\alpha_4\beta_7$+ expression by standard flow cytometry using the FACS Calibur system.

2.6. Generation and production of rhesus recombinant $\alpha_4\beta_7$ monoclonal antibody (Rh-$\alpha_4\beta_7$ mAb)

Immunoglobulin heavy and light chain variable regions were synthesized as minigenes comprising complementarity determining regions of murine $\alpha_4\beta_7$ mAb [26], and human heavy and light chain variable region framework sequences. Synthesized variable region minigenes were subcloned into expression vectors containing rhesus IgG1 heavy chain or rhesus kappa light chain constant region sequences.

For large scale production of recombinant antibody, recombinant heavy and light chain vectors were packaged in retroviral vectors and used to infect CHO cells using the GPEx® expression technology (Catalent Pharma Solutions, Middleton, WI). A pool of transduced cells was grown in serum free medium and secreted antibody purified by protein A affinity chromatography. The purified Rh-$\alpha_4\beta_7$ mAb was placed in phosphate buffer, pH 6.5, and confirmed to contain <1 EU/mg of antibody.

2.7. Characterization of recombinant Rh-$\alpha_4\beta_7$ mAb

Specificity of Rh-$\alpha_4\beta_7$ was confirmed by cross-blocking experiments. Briefly, $\alpha_4\beta_7$+ expressing Hut 78 cells were incubated with varying concentrations of Act I or a control mouse antibody. After washing, cells were stained with the recombinant Rh-$\alpha_4\beta_7$ conjugated to the fluorophore APC. Affinity of recombinant Rh-$\alpha_4\beta_7$ was compared to the murine $\alpha_4\beta_7$ mAb by incubating serial dilutions of both antibodies with a fixed number of Hut 78 cells and measuring antibody concentration before and after incubation. The affinity constant (K_d) for each antibody was calculated as previously described [36]. Similar cross-blocking experiments were performed on PBMC isolated from uninfected RM.

2.8. Detection of cell bound Rh-$\alpha_4\beta_7$ following in vivo treatment of RM

Aliquots of PBMC and intra-epithelial lymphocytes isolated from heparinized blood and rectal biopsy samples, respectively, were stained with the biotinylated murine $\alpha_4\beta_7$ mAb followed by streptavidin PE-Cy7 to determine if the murine $\alpha_4\beta_7$ mAb binding was blocked by the Rh-$\alpha_4\beta_7$ mAb *in vivo*. To determine if decreases in levels of $\alpha_4\beta_7$+ lymphocytes as detected by the murine $\alpha_4\beta_7$ mAb were due to depletion or blocking, an aliquot of the same cells were also stained with anti-α_4 integrin-PE or anti-β_7 integrin-APC which recognize epitopes distinct from the murine $\alpha_4\beta_7$ and Rh-$\alpha_4\beta_7$ mAbs. Since α_4 integrin-PE+ lymphocytes also include $\alpha_4\beta_1$+ lymphocyte populations, the data shown herein includes staining with β_7 integrin-APC only, since cells bound by this Ab would most likely represent the same population detected by the murine $\alpha_4\beta_7$ and the Rh-$\alpha_4\beta_7$ mAbs.

2.9. Measurement of plasma levels of Rh-$\alpha_4\beta_7$

Levels of rhesus recombinant Rh-$\alpha_4\beta_7$ antibody in monkey plasma were measured using the $\alpha_4\beta_7$+ expressing CD8+ human T-cell line, HuT 78 in a flow cytometry-based assay. Plasma obtained from each monkey before and after Rh-$\alpha_4\beta_7$ mAb administration was serially diluted in PBS/2% FBS and incubated with 10^6 HuT 78 cells for 30 min. Cells were then washed twice with PBS and incubated for 30 min with polyclonal goat anti-human IgG-PE (Jackson ImmunoResearch, West Grove, PA) that had been shown to cross react with rhesus IgG. Cells were washed twice with PBS and fixed with PBS/2% formalin. Stained cells were analyzed on a FACS Calibur flow cytometer for PE fluorescence. The mean channel fluorescence intensity (MFI) of cells stained with monkey serum was compared to MFI of cells stained with known concentrations of the Rh-$\alpha_4\beta_7$ mAb. Whenever possible, the mean of two measurements made at different serum dilutions was used. The sensitivity of this assay was <4 μg/ml.

2.10. Statistical analysis

Data are represented as means ± standard deviation (SD) and were analyzed by using the two-tailed Student's *t* test. A *P* value of <0.05 was considered to be statistically significant.

3. Results

3.1. Characterization of $\alpha_4\beta_7$ expression in cell lineages from RM

Previous characterization of $\alpha_4\beta_7$ on human leukocytes using the murine Act1 mAb has shown this mAb to specifically recognize the $\alpha_4\beta_7$ heterodimer [10,26]. These studies showed that while T-cells and B-cells express both $\alpha_4\beta_7^{low}$ and $\alpha_4\beta_7^{high}$ populations, NK cells exhibited a predominantly $\alpha_4\beta_7^{low}$ phenotype. Previous studies have also examined the induction of $\alpha_4\beta_7$ expression on SIV-specific CD8+ T-cells in RM [37,38], but to date, a comprehensive analysis of profiles of $\alpha_4\beta_7$-expressing cell lineages and their subsets from RM has been lacking. Our laboratory therefore set out to first characterize $\alpha_4\beta_7$ expression profiles on T-cell and its subsets, B-cells and NK cell subsets isolated from healthy uninfected RM. Using multi-parameter flow cytometry, the biotinylated murine $\alpha_4\beta_7$ mAb was tested for reactivity along with a panel of mAb reagents that have previously been shown by several labs including ours to be optimal for the identification of the aforementioned cell populations in the PBMC samples from 9 uninfected RM. It should be noted that high and low densities of $\alpha_4\beta_7$+ expression were more discernable on the FACS Calibur flow cytometer while an overlay of histograms was necessary to better identify these two sub-populations on the LSRII flow cytometer. This is likely due to basic system differences between these two flow cytometry instruments such as laser voltages or compensation settings, but it is important to note that the frequencies of $\alpha_4\beta_7$+ lymphocytes acquired by the two flow cytometers was still similar, if not identical. As shown by the representative FACS profiles in Fig. 1A, the analysis of NK cells (defined as CD3−CD8+CD14−CD20−NKG2A+) and their subsets based on CD16 and CD56 expression [34] revealed that, in agreement with the previous characterization of human NK cells, >50% total RM NK cells generally expressed low mean densities of $\alpha_4\beta_7$ with the majority of $\alpha_4\beta_7$+ cells being the cyto-

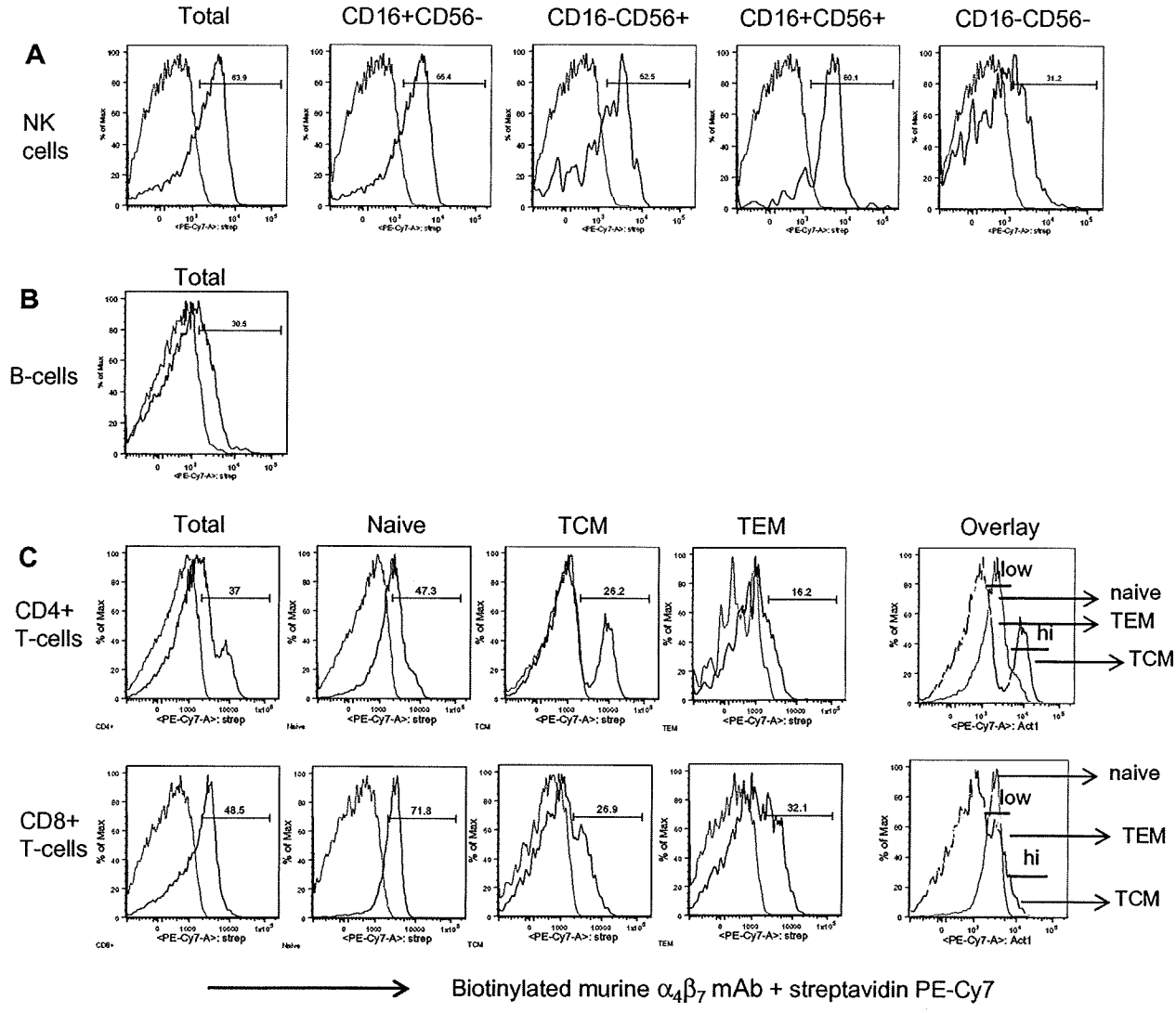

Fig. 1. Representative LSR II facilitated flow cytometric profiles of $\alpha_4\beta_7$ expression on total and subset populations of (A) NK cells, (B) B-cells and (C) T-cell lineages in PBMC from 9 healthy uninfected RM. For detection of $\alpha_4\beta_7$+ cells, PBMC from 9 RM were surface stained with biotinylated murine $\alpha_4\beta_7$ mAb followed by secondary staining with streptavidin PE-Cy7. Shown is representative data ($n = 9$ RM) with gating indicating $\alpha_4\beta_7$+ populations in comparison to background levels. To better indicate $\alpha_4\beta_7^{low}$ and $\alpha_4\beta_7^{high}$ densities, (C) also includes an overlay of $\alpha_4\beta_7$+ naïve, $\alpha_4\beta_7$+ TCM and $\alpha_4\beta_7$+ TEM for CD4+ and CD8+ T-cells.

kine-producing CD16+/CD56+ and the cytolytic CD16+CD56− NK cell subsets (Table 1). Low relative densities of $\alpha_4\beta_7$ expression were also observed on the CD16−CD56− NK cell subset in RM. In contrast to what has been reported for human B-cells, $\alpha_4\beta_7$ expression on the majority of B-cells (Fig. 1B, Table 1) in RM was found to be $\alpha_4\beta_7^{low}$. With regard to T-cells, greater than 35% of both CD4+ and CD8+ T-cells from healthy uninfected RM were found to express $\alpha_4\beta_7$ with CD4+ T-cells exhibiting both $\alpha_4\beta_7^{low}$ and $\alpha_4\beta_7^{high}$ phenotypes (Fig. 1C). Further gating based on CD28 and CD95 expression to distinguish naïve (CD28+CD95−), TCM (CD28+ CD95+) and TEM (CD28−CD95+) subsets in the periphery revealed that while there was clearly a discrete sub-population of $\alpha_4\beta_7^{high}$ expressing CD4+ TCM cells, the naïve and TEM CD4+ T-cells were $\alpha_4\beta_7^{low}$. All three (naïve, TCM and TEM) CD8+ T-cell subsets appeared to exhibit a $\alpha_4\beta_7^{low}$ phenotype (Fig. 1C). The average frequencies of $\alpha_4\beta_7$+ cells for each cell lineage and its subsets in the periphery of uninfected RM are summarized in Table 1. The examination of $\alpha_4\beta_7$ expression in intra-epithelial lymphocytes isolated from jejunum, colon and rectal tissue samples from two healthy uninfected RM (Fig. 2, representative data) revealed a predominantly $\alpha_4\beta_7^{low}$ phenotype on CD4+ T-cells, with the exception of CD4+ memory cells, which expressed heterogeneous levels of $\alpha_4\beta_7^{high}$ and were higher in frequency in the cells from the colon and rectum as compared with jejunum biopsies. CD8+ T-cells and its subsets from these tissue samples exhibited a predominantly $\alpha_4\beta_7^{low}$ phenotype (not shown).

The expression of $\alpha_4\beta_7^{high}$ on CD4+ memory T-cells has been described before and more recent studies have demonstrated that the frequency of CD4+ T-cells that express $\alpha_4\beta_7^{high}$ can be significantly increased *in vitro* via activation in the presence of retinoic acid [27,29,31], which is a vitamin A metabolite believed to be responsible for promoting the gut-homing of lymphocytes *in vivo*. In order to determine if this held true for RM T-cells, purified CD4+ T-cells were cultured *in vitro* with low levels of IL-2 and/or activated with anti-CD3/CD28 Ab-conjugated magnetic beads in the presence or absence of all-trans RA. As shown in Fig. 3A and B, flow

Table 1
Frequency (Mean ± SD) of $\alpha_4\beta_7$+ cells in major cell lineages and their subsets* in PBMC isolated from healthy uninfected RM ($n = 9$).

Cell sub-population	Frequency of $\alpha_4\beta_7$+ lymphocytes detected using murine $\alpha_4\beta_7$ mAb
CD3+CD4+ T-cells	51.9 ± 1.5
Na	66.7 ± 20.9
TCM	31.6 ± 6.2
TEM	18.9 ± 6.7
CD3+CD8+ T-cells	60.6 ± 16.8
Na	83.1 ± 13.4
TCM	34.4 ± 12.6
TEM	44.8 ± 15.2
CD3−CD20+ B-cells	48.5 ± 12.8
CD3−CD8+ NKG2A+ NK cells	68.2 ± 14.8
CD16−CD56+	68.7 ± 17.6
CD16+CD56−	77.4 ± 19.6
CD16−CD56−	47.0 ± 29.8
CD16+CD56+	73.2 ± 9.8

* RM lymphocytes were gated for the specific population (such as gated on CD3+CD4+ T-cells) for analysis of the frequency of $\alpha_4\beta_7$+ cells within each sub-population.

cytometric analysis on the FACS Calibur revealed that when compared to resting CD4+ T-cells, the effect of RA on $\alpha_4\beta_7$ expression was minimally enhanced when CD4+ T-cells were cultured with only IL-2. However, a dramatic increase (~4-fold) in the frequency of $\alpha_4\beta_7^{high}$ CD4+ T-cells was observed when these lymphocytes were activated in the presence of RA for 5 days. The induction of $\alpha_4\beta_7$ on CD8+ T-cells following incubation with RA was also examined but was not found to be significant, with activated cells exhibiting a less than twofold increase in the frequency of $\alpha_4\beta_7^{high}$ CD8+ T-cells in the presence of RA for 5 days (data not shown). Thus, these data collectively demonstrate that $\alpha_4\beta_7$ expression on RM lymphocytes can be readily identified and results largely reflect $\alpha_4\beta_7$ expression patterns similar to those noted for human lymphocytes. Furthermore, RA can be utilized successfully to manipulate and upregulate and potentially prepare large numbers of $\alpha_4\beta_7$+ expressing CD4+ T for autologous therapeutic transfusion studies.

3.2. In vivo administration of Rh-$\alpha_4\beta_7$ mAb results in a significant decline in the level of $\alpha_4\beta_7$+ lymphocytes in the periphery and GI tissues

The findings that the murine $\alpha_4\beta_7$ mAb effectively cross-reacts with $\alpha_4\beta_7$+ lymphocytes from RM prompted us to determine whether $\alpha_4\beta_7$-expressing lymphocytes could be targeted *in vivo*. In order to minimize the immunogenicity of the murine $\alpha_4\beta_7$ mAb *in vivo*, a rhesus recombinant IgG1 antibody was generated as noted in Section 2. The recombinant Rh-$\alpha_4\beta_7$ mAb was then confirmed by flow cytometry to exhibit specificity that was similar to murine $\alpha_4\beta_7$ mAb. The human $\alpha_4\beta_7$-expressing cell line, Hut 78, was used to characterize Rh-$\alpha_4\beta_7$ mAb. The Rh-$\alpha_4\beta_7$ mAb bound to Hut 78 cells and could be completely cross-blocked by the pre-incubation of cells with the parent murine $\alpha_4\beta_7$ mAb (Fig. 4A). The affinity constant for Rh-$\alpha_4\beta_7$ was similar to the murine $\alpha_4\beta_7$ mAb when measured by binding to Hut 78 cells with K_d values of 6.4×10^{-10} and 1.8×10^{-10} for Rh-$\alpha_4\beta_7$ mAb and murine $\alpha_4\beta_7$ mAb, respectively. The specificity of Rh-$\alpha_4\beta_7$ mAb was further confirmed by the finding that pre-incubation of RM PBMC with Rh-$\alpha_4\beta_7$ was cross-blocked the binding of murine $\alpha_4\beta_7$ mAb by almost 100% *in vitro* (and vice versa). Of interest was the finding that the pre-incubation with Rh-$\alpha_4\beta_7$ resulted in minimal cross-blocking of anti-β_7 integrin mAb (Fig. 4B) or anti-CD49d (α_4, data not shown) single chain specific mAb. Also of interest is our observation that

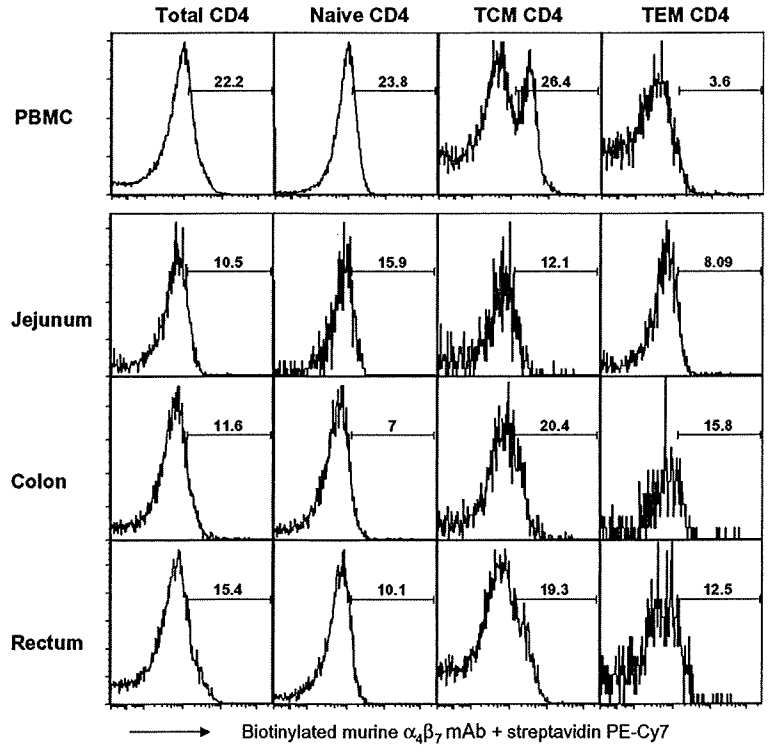

Fig. 2. Representative flow cytometric profiles of $\alpha_4\beta_7$ expression on total and subset populations of CD4+ T-cells in the gut of healthy RM. Intra-epithelial lymphocytes were isolated from colon, jejunum and rectal tissue samples from 2 healthy uninfected RM. The frequency of $\alpha_4\beta_7$+ lymphocytes were determined on the LSR II as described in the text. The number noted within each profile indicates only the frequency of cells expressing $\alpha_4\beta_7^{high}$ densities. Shown for comparison are $\alpha_4\beta_7^{high}$ populations in CD4+ T-cell subsets from uninfected RM PBMC.

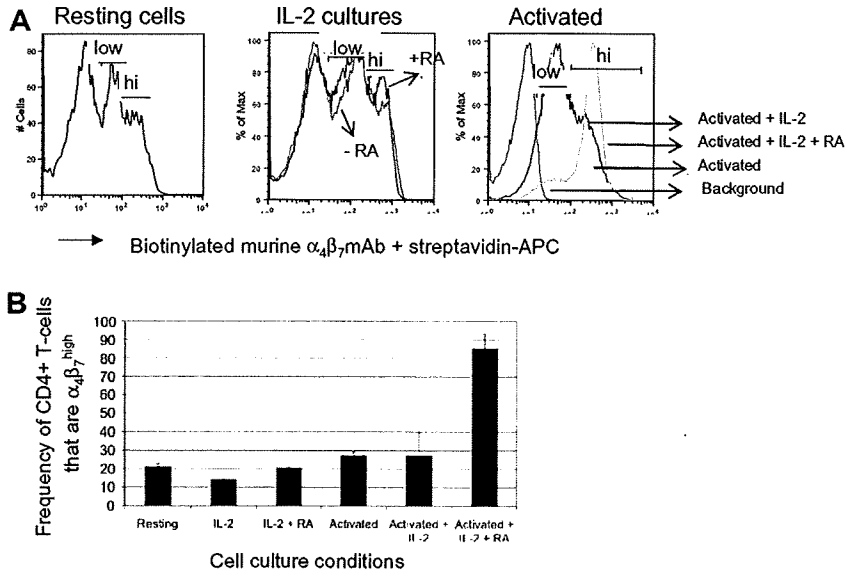

Fig. 3. Retinoic acid (RA) induces $\alpha_4\beta_7$ expression on CD4+ T-cells. (A) Representative flow cytometry profiles (acquired by the FACS Calibur) of $\alpha_4\beta_7$ expression on resting CD4+ T-cells and CD4+ T-cells cultured or activated in media containing 50 U/ml IL-2 or 10 nM retinoic acid (RA). Gating was performed on viable cells only. (B) Bar chart illustrating the frequency (Mean ± SD) of $\alpha_4\beta_7^{high}$ CD4+ T-cells under indicated conditions. The assay was repeated three times and performed using purified CD4+ T-cells from 2 RM each time.

staining with anti-β_7 integrin mAb alone did not reveal distinct low and high density β_7+ expressing CD4+ T-cell sub-populations as seen by staining with Rh-$\alpha_4\beta_7$ or murine $\alpha_4\beta_7$ mAbs. Collectively, these data suggest that the Rh-$\alpha_4\beta_7$ mAb is directed at an epitope formed by the $\alpha_4\beta_7$ heterodimer which is distinct from those that are recognized by the individual α_4 or β_7 mAbs. This finding was exploited for the detection of cells bound by Rh-$\alpha_4\beta_7$ *in vivo* (see Section 2 and below).

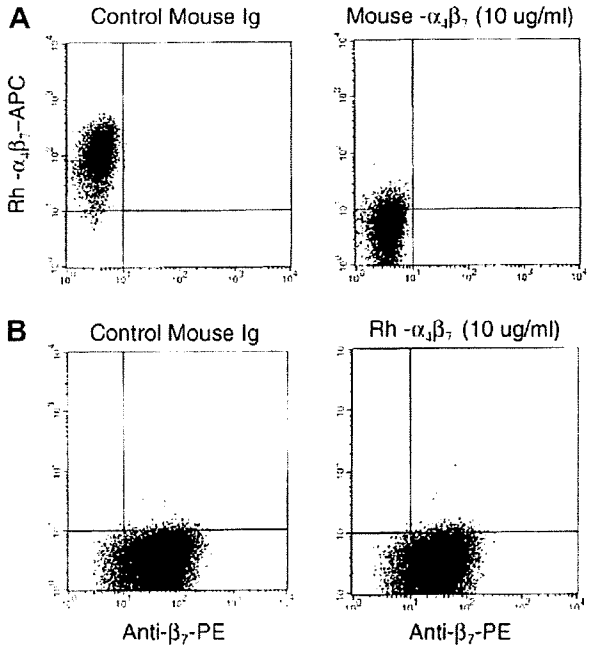

Fig. 4. Recombinant rhesus $\alpha_4\beta_7$ (Rh-$\alpha_4\beta_7$) is cross-blocked by murine $\alpha_4\beta_7$ mAb but not β_7 mAb. (A) Hut 78 cells were pre-incubated with mouse isotype control antibody (left panel), or with murine $\alpha_4\beta_7$ mAb followed by staining with Rh-$\alpha_4\beta_7$-APC. (B) Hut 78 cells were pre-incubated with mouse isotype control antibody (left panel) or with rhesus $\alpha_4\beta7$ followed by staining with β_7-PE mAb.

Having characterized the binding and specificity properties of Rh-$\alpha_4\beta_7$, an acute *in vivo* administration study was then initiated in two healthy uninfected RM RFm10 and RFn10 (6.49 and 7.17 kg, respectively). The Rh-$\alpha_4\beta_7$ mAb was diluted in sterile infusion-grade saline and was gradually administered intravenously (IV) to each of the two animals at a dose of 50 mg/kg, which equates to a starting dose of 0.85 mg/ml of plasma based on the assumption that each RM has approximately 60 ml blood/kg. The monkeys demonstrated no adverse effects during or after the antibody infusion. Blood samples used for PBMC isolation, cell blood counts (CBC) and blood chemistries were collected at baseline and at days 1, 5, 8, 14, 22, 29, 36, 43, 56 and 63 post infusion. As evident by the representative blood chemistries results (Supplemental data, Table 1), Rh-$\alpha_4\beta_7$ was well tolerated by both animals and did not lead to any significant physiological changes. The plasma levels of Rh-$\alpha_4\beta_7$ were also determined over the course of the study (see Fig. 5) and were found to be at a maximum as expected on Day 1 (603 and 676 μg/ml in RFm10 and RFn10, respectively) followed by a decline thereafter with an alpha half life of approximately 8 days. By day 29, notable concentrations were still detected in plasma from both RFm10 (45 μg/ml) and RFn10 (35 μg/ml) but undetectable levels were noted by day 56.

PBMC were analyzed by flow cytometry to determine the frequency of major $\alpha_4\beta_7$+ cell lineages and their subsets. Detection of $\alpha_4\beta_7$+ cells following *in vivo* administration of the Rh-$\alpha_4\beta_7$ using the parent murine $\alpha_4\beta_7$ mAb alone would not be feasible due to cross-blocking. Attempts were made to directly detect Rh-$\alpha_4\beta_7$ on PBMC utilizing PE-conjugated anti-rhesus IgG. However, despite Fc blocking prior to *in vitro* staining, the background level with this secondary antibody was too high to allow for clear identification of cells bound by the Rh-$\alpha_4\beta_7$ (data not shown). Based on the findings that the Rh- $\alpha_4\beta_7$ mAb does not block the reactivity of mAb against either the α_4 intergrin or β_7 integrin single chain, it was reasoned that use of the anti-β_7 integrin mAb would be preferable since the anti-α_4 integrin mAb would not only bind to cells with bound Rh-$\alpha_4\beta_7$ but would also bind to cells that express $\alpha_4\beta_1$. It was thus reasoned that the detection of cells that are β_7+ would likely represent cells that are bound with the Rh-$\alpha_4\beta_7$ mAb *in vivo*. Thus, the frequency of $\alpha_4\beta_7$+ cells was determined by staining aliquots of

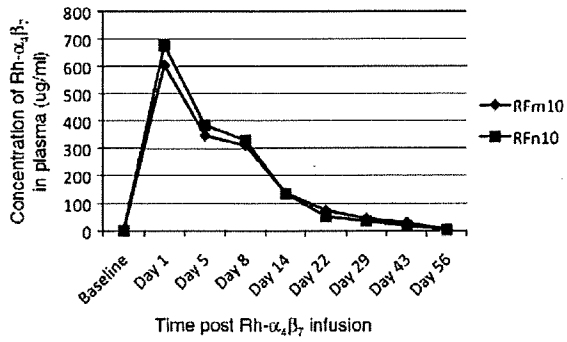

Fig. 5. Plasma concentrations of Rh-$\alpha_4\beta_7$ following *in vivo* infusion. Plasma was isolated from heparinized blood at the indicated time points from animals RFm10 and RFn10 and the levels of Rh-$\alpha_4\beta_7$ mAb were measured using the $\alpha_4\beta_7$+ expressing CD8+ human T-cell line HuT 78 in a flow cytometry-based assay. The concentration of Rh-$\alpha_4\beta_7$ in each plasma sample was determined by comparing the MFI of HuT 78 cells stained with monkey plasma to the MFI of HuT 78 cells stained with known concentrations of Rh-$\alpha_4\beta_7$ mAb.

cells with the parent murine $\alpha_4\beta_7$ mAb as well as with anti-β_7 chain specific mAb. Results revealed that on Day 1 post infusion, there was significant cross-blocking of $\alpha_4\beta_7$+ T-cells and α_4v_7+ NK cells by Rh-$\alpha_4\beta_7$ mAb because staining of PBMC with the parent murine $\alpha_4\beta_7$ mAb showed a decline in frequency by ~95% while the decline in the frequency of $\alpha_4\beta_7$+ B-cells was by ~80% in both the monkeys (Fig. 6A, upper left panel). This decline occurred in both $\alpha_4\beta_7^{low}$ and $\alpha_4\beta_7^{high}$ subsets. The frequency of $\alpha_4\beta_7$+ lymphocytes remained low through Day 22 until a significant increase to levels near baseline were noted by Day 43.

To distinguish between cross-blocking and a true decline in $\alpha_4\beta_7$+ lymphocytes, staining with anti-β_7 mAb was performed and also revealed a similar decline in β_7+ lymphocytes on Day 1 post infusion (Fig. 6A, lower left panel). However, this was followed by a rebound to ~60–70% of baseline on Day 5. These increased values were maintained until day 22 with values returning near baseline by Day 36. These data suggest that while there is an initial and partial decline in the $\alpha_4\beta_7$+ expressing cells, this is followed by a recovery of cells that express $\alpha_4\beta_7$+ but are blocked by the *in vivo* presence of the Rh-$\alpha_4\beta_7$ mAb. The absolute

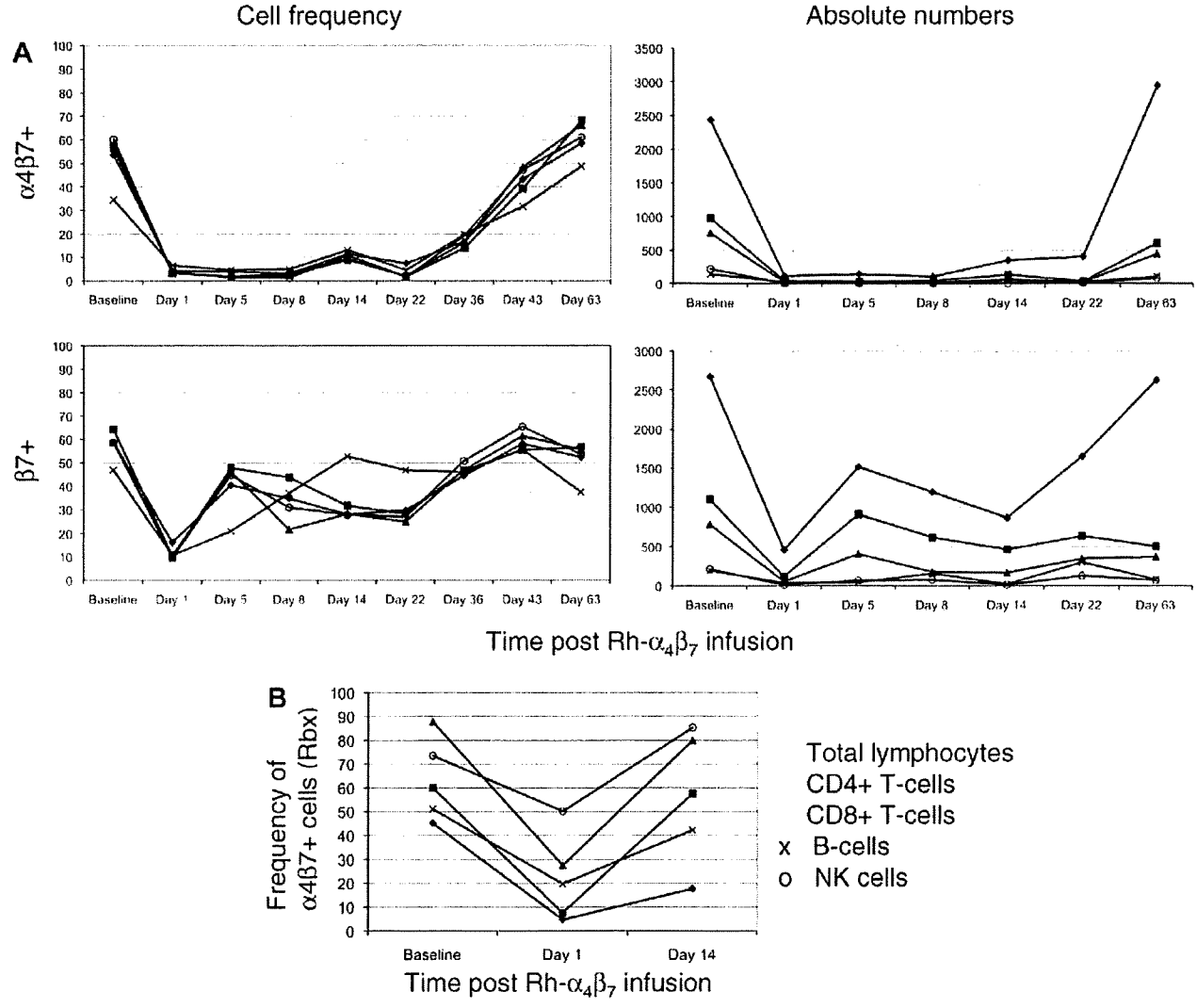

Fig. 6. *In vivo* administration of Rh-$\alpha_4\beta_7$ leads to significant decline and subsequent cross-blocking of $\alpha_4\beta_7$+ lymphocytes. Rh-$\alpha_4\beta_7$ was infused IV at a dose of 50 mg/kg to 2 RM and the frequency and ABS of $\alpha_4\beta_7$+ and β_7+ lymphocytes for each cell lineage in (A) the periphery and (B) Rbx, were determined at the indicated points post infusion. Shown is representative data for total $\alpha_4\beta_7$+ lymphocytes (♦), $\alpha_4\beta_7$+ CD4+ T-cells (■), $\alpha_4\beta_7$+ CD8+ T-cells (▲), $\alpha_4\beta_7$+ B-cells (x), and $\alpha_4\beta_7$+ NK cells (o).

numbers (ABS) of total lymphocytes, CD4+ T-cells, CD8+ T-cells, B-cells and NK cells expressing $\alpha_4\beta_7$+ and β_7+ (Fig. 6A, right panels) were also calculated in order to distinguish whether the observed decreases in cell frequency were due to the cross-blocking effects of Rh-$\alpha_4\beta_7$ mAb or was due to a true decrease (depletion or re-distribution). As shown by the representative data in Fig. 6A, the analysis of ABS of $\alpha_4\beta_7$+ and β_7+ T-cells, B-cells and NK cells revealed a true decline in these cell populations in the periphery on Day 1 which reflects the cell frequency data. By day 63, the ABS of all these lymphocyte subsets returned to baseline levels.

Since $\alpha_4\beta_7$+ lymphocytes home to the GI tract which is the target site of interest, the frequency of $\alpha_4\beta_7$+ and β_7+ lymphocytes was also determined in rectal biopsy (Rbx) samples from each animal at baseline, Day 1 and Day 14 post infusion with the Rh-$\alpha_4\beta_7$ mAb. A similar analysis of BM and BAL samples was also performed to determine the extent of Rh-$\alpha_4\beta_7$ bio-distribution *in vivo*. As shown by the results in Fig. 6B, staining of isolated day 1 Rbx intra-epithileal lymphocytes with either the murine $\alpha_4\beta_7$ mAb or the anti-β_7 integrin mAb revealed a 10-fold and 3-fold decline in the frequency of $\alpha_4\beta_7$+ CD4+ T-cells and $\alpha_4\beta_7$+ CD8+ T-cells, respectively. An approximately 2-fold decrease was also noted for $\alpha_4\beta_7$+ B-cells and $\alpha_4\beta_7$+ NK cells in such Rbx tissues. By Day 14, the frequencies of all $\alpha_4\beta_7$+ lymphocyte populations were at or near baseline. A similar pattern of decrease in the frequency of $\alpha_4\beta_7$+ lymphocytes was noted for bone marrow samples in that significant declines in $\alpha_4\beta_7$+ lymphocytes were observed on Day 1 while a recovery to levels near baseline were noted on Day 14. Data obtained from BAL samples did not reveal any clear trend (data not shown). In summary, *in vivo* administration of a single dose of 50 mg/kg of Rh-$\alpha_4\beta_7$ was well tolerated and resulted in significant initial decline and a prolonged blocking of the $\alpha_4\beta_7$ molecule on peripheral $\alpha_4\beta_7$+ T-cells, B-cells and NK cells for a significant period of time (up to 5 weeks) as well as a substantial decrease in the frequency of these lymphocyte subsets in Rbx and BM samples, but for a more transient time period.

3.3. Cross-sectional and longitudinal analyses of uninfected and SIV-infected RM reveals early changes in the frequency and absolute numbers (ABS) of select $\alpha_4\beta_7$+ lymphocyte subsets during the acute stage of infection

Since our main goal is to eventually administer the Rh-$\alpha_4\beta_7$ mAb to RM prior to or during acute SIV-infection, it was deemed important to first characterize and understand the changes, if any, that occur in $\alpha_4\beta_7$+ lymphocytes following SIV-infection. To this end, both longitudinal and cross-sectional studies were conducted to evaluate the acute and chronic effects, respectively, of SIV-infection on $\alpha_4\beta_7$+ expression on lymphocytes from the periphery and GI tissues of uninfected and SIV-infected RM. The cross-sectional analysis of PBMC samples from SIVmac239 chronically infected RM ($n = 9$) with either high VL (>100,000 vRNA copies/ml plasma, $n = 5$) or low VL (<10,000 vRNA copiles/ml plasma, $n = 4$) and for comparison uninfected RM ($n = 5$) failed to reveal any significant changes ($p > 0.05$) in the frequency of $\alpha_4\beta_7$+ T-cell subsets, $\alpha_4\beta_7$+ B-cells or $\alpha_4\beta_7$+ NK cell subsets in samples from the SIV-infected animals during chronic infection as compared to the uninfected control animals (data not shown). However, the comparison of intra-epithelial lymphocytes isolated from Rbx from 2 uninfected and 2 SIV-infected RM 8–10 weeks post infection revealed a $\geqslant$2-fold decline in the frequency of $\alpha_4\beta_7$+ NK cells and $\alpha_4\beta_7$+ T-cells particularly among $\alpha_4\beta_7$+ CD4+ TEM cells and $\alpha_4\beta_7$+ CD8+ T-cells (Fig. 7) while a relatively smaller decline was noted for $\alpha_4\beta_7$+ B-cells in these Rbx tissues. The relative viral loads in enriched populations of $\alpha_4\beta_7$+ versus $\alpha_4\beta_7$– enriched CD4+ T-cell populations isolated from the peripheral blood of 6 chronically SIV-infected but asymptomatic RM with both high and low ($n = 3$ each) plasma VL was also determined but results revealed no statistically significant differences in cellular VL copy number between the $\alpha_4\beta_7$+ and $\alpha_4\beta_7$– CD4+ T-cells ($p > 0.05$, data not shown).

In contrast to chronically SIV-infected RM, significant changes in the frequency and ABS of select peripheral T-cell and NK cell subsets were noted during the acute phase of SIV-infection. Analysis of 4 RM prior to (following two consecutive baseline values) and during the first 5 weeks of infection with SIVmac239 revealed that a significant increase in both the frequency (Fig. 8A, left panel) and ABS (not shown) of total NK cells occurred in the periphery which is similar to our previous findings [34]. Analysis of the specific $\alpha_4\beta_7$+ NK cells and its subsets (Fig. 8A, right panel) revealed that a nearly 4-fold decline occurred in the frequency of $\alpha_4\beta_7$+ CD16–CD56+ and $\alpha_4\beta_7$+ CD16–CD56– NK subsets at week 1 post infection while a less significant decline was also noted in the frequency of $\alpha_4\beta_7$-expressing CD16+CD56– and CD16+CD56+ NK subsets. The determination of absolute numbers (ABS) revealed an approximate 2-fold decline by week 2 and the ABS of the $\alpha_4\beta_7$+ CD16–CD56+ and $\alpha_4\beta_7$+ CD16–CD56– NK subsets remained low through week 5 (not shown). However, a substantial increase in the ABS of $\alpha_4\beta_7$+ CD16+CD56– and CD16+CD56+ NK subsets was observed, with a 4-fold and 2-fold increase, respectively, being

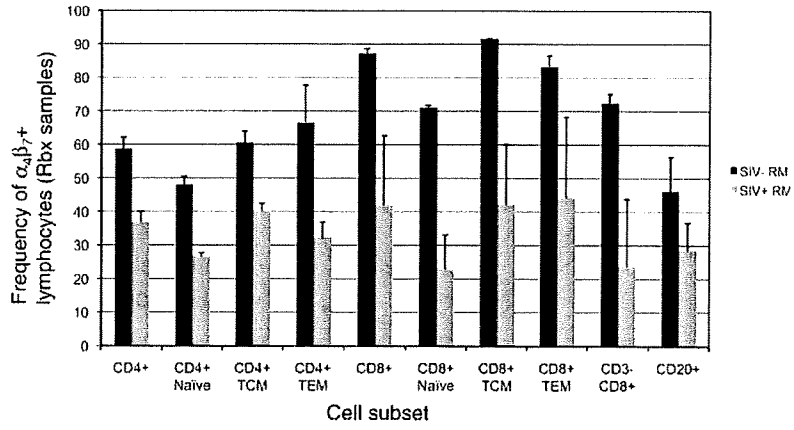

Fig. 7. Chronic SIV infection in RM leads to a decline in the frequency of most $\alpha_4\beta_7$+ lymphocytes in the GALT. Intra-epithelial lymphocytes isolated from rectal biopsy samples from uninfected (black bars, $n = 2$) and SIV-infected rhesus macaques (grey bars, $n = 2$, approximately 2 mths post infection) were stained with biotinylated murine $\alpha_4\beta_7$ mAb and streptavidin-PE-Cy7 and analyzed by flow cytometry. Shown are the frequency of $\alpha_4\beta_7$+ cells within CD4+ and CD8+ T-cell subsets, NK cells and B-cells.